haematologica
Journal of The Ferrata Storti Foundation

Atherogenic lipid stress induces platelet hyperactivity through CD36-mediated hyposensitivity to prostacyclin – the role of phosphodiesterase 3A

by Martin Berger, Zaher Raslan, Ahmed Aburima, Simbarashe Magwenzi, Katie S. Wraith, Benjamin E.J. SPurgeon, Matthew S. Hindle, Robert Law, Maria Febbraio, and Khalid M. Naseem

Haematologica 2019 [Epub ahead of print]

Citation: Martin Berger, Zaher Raslan, Ahmed Aburima, Simbarashe Magwenzi, Katie S. Wraith, Benjamin E.J. SPurgeon, Matthew S. Hindle, Robert Law, Maria Febbraio, and Khalid M. Naseem. Atherogenic lipid stress induces platelet hyperactivity through CD36-mediated hyposensitivity to prostacyclin – the role of phosphodiesterase 3A. Haematologica. 2019; 104:xxx doi:10.3324/haematol.2018.213348

Atherogenic lipid stress induces platelet hyperactivity through CD36-mediated hyposensitivity to prostacyclin – the role of phosphodiesterase 3A.

Martin Berger[1,2,3], Zaher Raslan[3*], Ahmed Aburima[1*], Simbarashe Magwenzi[1], Katie S. Wraith[1], Benjamin E.J. Spurgeon[3], Matthew S. Hindle[3], Robert Law[1], Maria Febbraio[4] & Khalid M. Naseem[1,3]

[1]Centre for Cardiovascular and Metabolic Research, Hull York Medical School, University of Hull, Hull, UK.
[2] Department of Internal Medicine 1, University Hospital RWTH Aachen, Aachen, Germany.
[3] Discovery and Translational Science Department, Leeds Institute of Cardiovascular and Metabolic Medicine, University of Leeds, Leeds UK.
[4] School of Dentistry, University of Alberta, Edmonton, T6G 2R3, Canada.

* denotes equal contribution to study

Article type: original article
Running head: CD36 activates platelet PDE3A

Author for correspondence: Khalid M Naseem, Discovery and Translational Science Department, Leeds Institute of Cardiovascular & Metabolic Medicine, The LIGHT Laboratories, Clarendon Way, University of Leeds, Leeds LS2 9NL
Tel: +44 1333 431560
E-mail: k.naseem@leeds.ac.uk

Word count: 3982

Acknowledgements
The authors would like to thank the British Heart Foundation (PG/13/90/20578, PG/12/49/29441 and RG/16/5/32250) and the Rotations-Program of the Medical faculty of RWTH Aachen University for funding this study.

ABSTRACT

Prostacyclin (PGI_2) controls platelet activation and thrombosis through a cyclic adenosine monophosphate (cAMP) signalling cascade. However, in patients with cardiovascular diseases this protective mechanism fails for reasons that are unclear. Using both pharmacological and genetic approaches we describe a mechanism by which oxidised low density lipoproteins (oxLDL) associated with dyslipidaemia promote platelet activation through impaired PGI_2 sensitivity and diminished cAMP signalling. In functional assays using human platelets, oxLDL modulated the inhibitory effects of PGI_2, but not a phosphodiesterase (PDE)-insensitive cAMP analogue, on platelet aggregation, granule secretion and *in vitro* thrombosis. Examination of the mechanism revealed that oxLDL promoted the hydrolysis of cAMP through the phosphorylation and activation of PDE3A, leading to diminished cAMP signalling. PDE3A activation by oxLDL required Src family kinases, Syk and protein kinase C. The effects of oxLDL on platelet function and cAMP signalling were blocked by pharmacological inhibition of CD36, mimicked by CD36-specific oxidised phospholipids and ablated in $CD36^{-/-}$ murine platelets. The injection of oxLDL into wild type mice strongly promoted $FeCl_3$ induced carotid thrombosis *in vivo*, which was prevented by pharmacological inhibition of PDE3A. Furthermore, blood from dyslipidaemic mice was associated with increased oxidative lipid stress, reduced platelet sensitivity to PGI_2 *ex vivo* and diminished PKA signalling. In contrast, platelet sensitivity to a PDE-resistant cAMP analogue remained normal. Genetic deletion of CD36, protected dyslipidaemic animals from PGI_2 hyposensitivity and restored PKA signalling. These data suggest that CD36 can translate atherogenic lipid stress into platelet hyperactivity through modulation of inhibitory cAMP signalling.

INTRODUCTION

Myocardial infarction (MI) is characterised by platelet-driven atherothrombotic events that lead to acute occlusion of a coronary vessel. Excessive platelet activation is controlled by endothelial derived nitric oxide (NO) and prostacyclin (PGI_2)[1], but action of these protective agents are overcome in MI by mechanisms that are yet to be elucidated. A key risk factor for MI is dyslipidaemia, which is strongly associated with a pro-thrombotic phenotype linked to atherothrombosis and platelet hyperactivity[2,3]. The blood of high-risk individuals with dyslipidemia is characterized by increased plasma lipid peroxides, with low density lipoproteins (LDL) serving as a highly abundant carriers for these oxidatively-modified lipids[4–6]. Oxidised LDL (oxLDL) are circulating pathological ligands that can enhance thrombosis through their ability to promote platelet hyperactivity. *In vitro* experimentation demonstrates that these modified lipoproteins can cause direct activation of platelets and also potentiate platelet activation induced by physiological agonists such as thrombin, ADP and epinephrine[7–10]. However, the potential pathophysiological importance of these observations for thrombosis *in vivo* remain unclear.

The scavenger receptor CD36 has emerged as a potential conduit for transducing plasma lipid stress into platelet hyperactivity and thrombosis, through the recognition of lipoprotein associated molecular patterns (LAMPs). CD36, alone or potentially in combination with Toll-Like Receptor (TLR)2 and TLR6 drive a complex series of intracellular signaling events that are associated with platelet activation[11–15]. Upon ligation of CD36, Src family kinases constitutively associated with the receptor, drive the activation of Syk, Vav-1, PLCγ2, ERK5 and JNK that are associated with platelet activation[13,16–18] More recently, data has emerged to suggest that the signalling events promote the generation of reactive oxygen species (ROS)[14,16,17]. ROS in turn activate ERK to drive thrombosis directly by platelet hyperactivity and caspase-dependent procoagulant activity[18,19]. Moreover, we found that ROS diminish sensitivity to the nitric oxide (NO)-stimulated cGMP-PKG inhibitory signaling cascade to reduce the threshold for platelet activation[17]. These data suggest that the translation of atherogenic lipid stress by platelet CD36 is functionally linked to both stimulation of activatory signalling pathways and to an as of yet ill-defined modulation of inhibitory pathways.

PGI_2 is the most potent endogenous regulator of platelet function with both genetic and pharmacological modulation of the pathway linked to accelerated thrombosis *in vivo*[20]. PGI_2 activates a cyclic adenosine monophosphate (cAMP) signalling pathway that leads to subsequent activation of protein kinase A (PKA) in platelets and results in the phosphorylation of numerous proteins[21], linked to the inhibition of Ca^{2+} mobilisation, dense granule secretion, spreading, integrin $\alpha_{IIb}\beta_3$ activation and aggregation *in vitro*[20]. To ensure optimal platelet function, cAMP levels are tightly regulated by the hydrolysing enzymes phosphodiesterase (PDE)2A and 3A. The pharmacological inhibition or genetic ablation of PDE3A in murine and human platelets reduces thrombotic potential[22,23]. Thus, factors that alter platelet inhibition by influencing cAMP synthesis or hydrolysis may be critical modulators of atherothrombosis and potentially lead to a pro-thrombotic phenotype. Given the established link between oxidised lipid stress and excessive platelet activation, the aim of this study was to determine if oxidatively modified lipoproteins could promote platelet hyperactivity through modulation of the PGI_2/cAMP signalling pathway.

METHODS

Reagents

Phospho-PKA Substrate (RRXS*/T*) Rabbit mAb and phospho-VASP-Ser$^{157/239}$ antibodies were from Cell Signaling Technology (Danvers, USA). PDE3A antibodies were from the MRC Unit (Dundee University, Scotland). Anti-β-Tubulin antibody was from Millipore (Nottingham, UK). BD Phosflow Lyse/Fix Buffer was from BD Biosciences (Oxford, UK). OxPC-E06 mAb was from Avanti Polar Lipids (Alabaster, USA). FITC-labeled Rat Anti-Mouse P-selectin (CD62P) and PE-labeled JON/A antibodies were from Emfret Analytics (Würzburg, Germany). Alexa-Fluor647 Goat anti-Rabbit IgG, Alexa-Fluor488 Succinimidyl Ester and Pacific-Blue Succinimidyl Ester were from ThermoFisher Scientific (Waltham, USA). PAR-1 peptide was from Anaspec (Fremont, USA). Anti-CD36 Antibody (FA6-152) was from Abcam (Cambridge, UK). Phosphodiesterase Activity Assay Kit was from Enzo Life Sciences (Exeter, UK). cAMP Biotrack EIA was from GE Healthcare (Buckinghamshire, UK). Horm Collagen was from Nycomed (Munich, Germany). PGI_2 and Cholesterol Assay Kit were from Cayman Chemical (Cambridge, UK). Vena8 Endothelial+ biochips were from Cellix (Hertfordshire, UK). All other reagents were from Sigma-Aldrich (Dorset, UK).

Experimental animals

$CD36^{-/-}$ mice were provided by Prof. Maria Febbraio (University of Alberta, Canada). C57BL/6 were from Charles River (Kent, UK). For high-fat diet studies, male mice were fed a 45% Western diet (Special Diet Services) for 12–16 weeks. Sex/age-matched littermates were fed a normal chow for the duration of the experiments and used as controls. For all remaining experiments male C57BL/6 and $CD36^{-/-}$ were used at 8 weeks of age.

Isolation and oxidation of plasma LDL

LDL (density 1.019–1.063 g/ml) was prepared from fresh human plasma by sequential density ultracentrifugation and oxidised with $CuSO_4$ (10 μmol/L)[14]. Separate preparations of LDL were used to repeat the individual experiments.

Platelet aggregation, flow assays, flow cytometric analysis, intravital microscopy, immunoprecipitation, immunoblotting, PDE activity assay and cAMP measurement.

Detailed methods are presented in the Supplemental methods.

Statistical analysis

Experimental data was analysed by Graphpad Prism 6 (La Jolla, USA). Data are presented as means±standard error of the mean (SEM) of at least 3 different experiments. Differences between groups were calculated using Mann-Whitney U Test or Kruskal-Wallis Test for non-parametric testing and statistical significance accepted at $p \leq 0.05$.

All studies were approved by the Hull York Medical school Ethics committee and University of Leeds Research Ethics committee.

RESULTS

Oxidised LDL causes platelet hyposensitivity to PGI_2.

Treatment of human washed platelets with PGI_2 (20 nM) for 1 minute, at a timepoint that induces maximal cAMP mediated signalling[24] reduced thrombin (0.05 U/ml)-induced aggregation from 89.0±4.1 to 9.4±4.4% ($p<0.01$) (Figure 1A). Next, platelets were treated with oxLDL or control native LDL (nLDL) (50 µg/ml) for 2 minutes prior to the addition of PGI_2 (20 nM) and thrombin (0.05 U/ml). The presence of oxLDL caused a partial recovery in thrombin-stimulated platelet aggregation to 50.0±9.3 ($p<0.015$ versus control), without stimulating aggregation directly (Figure 1A). In contrast, PGI_2-mediated inhibition was unaffected by nLDL (5.8±1.2%). Similar data was obtained when platelets were stimulated with collagen (Suppl. Figure 1). Next the effects of oxLDL in whole blood were examined. Stimulation of whole blood with PAR-1 peptide (10 µM) increased P-selectin expression, which was reduced by pre-treatment with PGI_2 (20 nM). Consistent with the aggregation experiments, oxLDL reduced inhibitory effects of PGI_2 (Figure 1B). Finally, the effects of oxLDL under physiological conditions of arterial flow were examined. Perfusion of whole blood over collagen coated biochips led to platelet deposition and thrombus formation (Figure 1Ci and ii), with surface coverage inhibited by PGI_2 (20nM) from 14.9±2.9 to 3.8±1.7% ($p<0.05$). OxLDL, but not nLDL, prevented PGI_2-mediated inhibition of platelet deposition (8.1±1.9%; $p<0.05$ compared to PGI_2 alone). OxLDL alone caused a small, but non-significant increase in thrombosis and was incorporated into the thrombi as evidenced by staining for oxidised lipid epitopes (Figure 1D). These data demonstrate that under a variety of different conditions oxLDL reduces platelet sensitivity to PGI_2.

Oxidised LDL modulates cAMP signalling through increased PDE3A activity.

PGI_2 inhibits platelets through the stimulation of cAMP-PKA signalling cascade.[20] Given the reduced platelet sensitivity to PGI_2, the direct effect of oxLDL on platelet cAMP metabolism were tested. Incubation with PGI_2 caused a significant increase in platelet cAMP concentrations (1814±166 fmol cAMP/1x10^8 platelets; $p<0.05$ versus basal). When platelets were treated with nLDL (50 µg/ml), the ability of the prostanoid to elevate cAMP was unaffected (1885±203 fmol cAMP/1x10^8 platelets), while oxLDL (50 µg/ml) prevented PGI_2-induced accumulation of cAMP (481±23 fmol cAMP/1x10^8 platelets; $p<0.05$ compared to PGI_2 alone) and also reduced basal cAMP concentrations (not significant) (Figure 2Ai). To determine if oxLDL blocked cAMP synthesis or accelerated cAMP breakdown by phosphodiesterase 3A (PDE3A) and PDE2[25],[25] the PDE2A inhibitor EHNA (20 µM) and the PDE3A inhibitor milrinone (10 µM) were used. Consistent with previous studies, both inhibitors potentiated cAMP accumulation in response to PGI_2.[28] [26] OxLDL reduced cAMP levels in the presence of EHNA (2645±122 to 488±7623 fmol cAMP/1x10^8 platelets, $p<0.05$), but failed to prevent cAMP accumulation in the presence of milrinone (4761±170 to 4386±15723 fmol cAMP/1x10^8 platelets $p<0.05$) (Figure 2Aii and 2Aiii). To confirm that the reduction in cAMP accumulation was not restricted to PGI_2, platelets were stimulated with forskolin, which increases cAMP in a receptor-independent non-compartmentalised mechanism. Forskolin (10 µM)-stimulated elevation in cAMP was prevented by preincubation with oxLDL (9506±526 to 4506±1136 fmol cAMP/2x10^8 platelets; $p < 0.05$) (Figure 2B).

Next, the effects of oxLDL on cAMP signalling were assessed. PGI_2 (50 nM) induced robust phosphorylation of a number of PKA substrates with apparent molecular weights of; 150, 100, 75, 70, 50, 37 and 20kDa (Figure 2C upper panel), and specifically vasodilator-stimulated phosphoprotein (VASP) (phosphoVASP-ser^{157}) (Figure 2C middle panel) an established target of PKA signalling[27]. These phosphorylation events were diminished by oxLDL (50 µg/ml), but unaffected by nLDL (50 µg/ml) (Figure 2Cii). To further establish that the reduced signalling response was due to enhanced cAMP hydrolysis, the experiment was repeated with 8-CPT-6-Phe-cAMP (50µM), a cell permeable non-hydrolysable (PDE resistant) analogue of cAMP (Suppl. Figure 2). Using a concentration that produced an equivalent quantity of intracellular cAMP (Suppl. Figure 3) as PGI_2 (50 nM), 8-

CPT-6-Phe-cAMP caused robust phosphorylation of PKA substrates, which were unaffected by oxLDL (Figure 2D). These data suggest that oxLDL may regulate platelet sensitivity to PGI_2 through modulation of the cAMP-signalling cascade by PDE3A.

CD36 is required for oxLDL modulation of cAMP signalling.

Previously, we and others, have shown that CD36 transduces the effects of oxLDL into platelet hyperactivity[14,18,28,29]. To examine the role of CD36 in linking oxLDL to altered cAMP signalling we used a three-pronged strategy; (i) the CD36 blocking antibody FA6-152, (ii) the oxidised phospholipid $oxPC_{CD36}$, a CD36-specific pathological ligand present in oxLDL,[26] and (iii) murine platelets deficient in CD36 (Suppl. Figure 4). This strategy, particularly the use of $oxPC_{CD36}$, previously to account for differences in human and murine platelet sensitivity to human oxLDL. PGI_2 induced a robust phosphorylation of both the preferred ser^{157} site and alternative PKA phosphorylation site ser^{239} in human platelets[30], which was reduced significantly by oxLDL. The presence of FA6-152 (1 μg/ml), but not control IgG (1 μg/ml), caused a significant recovery in phosphoVASP-ser^{157} (Figure 3A and B). $OxPC_{CD36}$ (25 μM), but not the control lipid, PAPC (25 μM), diminished phospoVASP-ser^{157} in response to PGI_2 (Figure 3C). Thrombin-induced aggregation of platelets isolated from WT and $CD36^{-/-}$ mice was indistinguishable and PGI_2 (20 nM) caused complete inhibition of aggregation with only shape change remaining (Figure 3D and E). However, in CD36-deficient platelets $oxPC_{CD36}$ (25 μM) did not influence the inhibitory effects of PGI_2 (Figure 3E). To confirm the mechanism underpinning these observations we examined cAMP signalling. PGI_2 (20 nM) caused a significant increase in cAMP in both WT and $CD36^{-/-}$ platelets (4382±175 and 4128±366 fmol cAMP/$1x10^8$ platelets). Preincubation with oxLDL, but not nLDL, reduced cAMP accumulation in WT mice (3347±294 fmol cAMP/$1x10^8$ platelets; $p<0.05$), but not $CD36^{-/-}$ (4196±224fmol cAMP/$1x10^8$ platelets) (Figure 3F). Furthermore, PGI_2 induced phosphoVASP-ser^{157} (Figure 3G) and ser^{239} (Suppl. Figure 5) was reduced by oxLDL in WT, but not $CD36^{-/-}$ platelets.

Atherogenic lipid stress induces platelet PDE3A activity through a mechanism that requires CD36, Src kinases and PKC.

Our data suggested that ligation of CD36 could activate PDE3A. We tested this directly measuring enzymatic activity of PDE3A immunoprecipitated from platelets treated with either oxLDL or $oxPC_{CD36}$. PDE activity in the immunoprecipitated samples was blocked by milrinone confirming enzyme activity was due to PDE3A (Suppl. Figure 6). OxLDL (10-100 μg/ml) caused a concentration-dependent increase in PDE3A activity (Figure 4Ai), which plateaued at 50 μg/ml (24±6.8%; $p<0.05$ compared to basal) and was maintained at 27.7%±8.5 above basal for up to 60 minutes (longest time tested) (Figure 4Aii). This was strikingly different from the physiological agonist thrombin which induced a rapid induction of PDE3A activity that peaked at 1 minute before returning to basal after 5 minutes (Suppl. Figure 7).

To link the sustained activation of PDE3A to decreased cAMP levels, we assessed the cyclic nucleotide concentrations over time. Platelets were incubated with oxLDL for up to 60 minutes, followed by a 1 minute treatment with PGI_2 (50nM) before measuring cAMP concentrations. The pre-incubation of platelets with oxLDL, but not nLDL (data not shown), for up to 60 minutes significantly blunted PGI_2 induced increases in cAMP with concentrations remaining at basal levels for the time course (Figure 4B). To confirm the role of CD36 in the activation of PDE3A, experiments were repeated with $oxPC_{CD36}$. In human platelets, $oxPC_{CD36}$ (25 μM), but not PAPC (25 μM), increased PDE3A activity (26.9±7.3%; $p<0.05$ compared to basal and PAPC) (Figure 4C). Critically, $oxPC_{CD36}$ stimulated activity in WT platelets to 25.4±2.4% ($p<0.05$ compared to basal or PAPC), but not in $CD36^{-/-}$ platelets (Figure 4D).

We previously described a CD36-specific signalling pathway that includes the sequential activation of Src-family

kinases (SFK), Syk, PLCγ2 and protein kinase C (PKC)[17] and investigated whether these kinases were involved in the activation of PDE3A. The non-selective SFK inhibitor, Dasatinib (10 μM), ablated $oxPC_{CD36}$-induced PDE3A activation (Figure 4E), while the Syk inhibitor, R406 (1 μM), caused significantly reduced PDE3A activity (Figure 4F). Given that CD36 signalling leads to PKC activation in a SFK manner and that PDE3A is a target of PKC in platelets[31], we tested the PKC inhibitors RO318220 (10 μM) and BIM1 (10 μM), and the intracellular Ca^{2+} chelator BAPTA-AM (20 μM) (Figure 4G). These three inhibitors blocked PDE3A activity induced by oxLDL, suggesting a PKC-dependent pathway ($p<0.05$). Platelet PDE3A activation is associated with phosphorylation of key serine residues[31]. We examined two of the most characterised sites, ser^{312} (PKA and PKC sensitive) and ser^{428} (PKC sensitive). OxLDL led to a time-dependent phosphorylation of ser^{428} which peaked at 2 minutes and was still evident at 10 minutes, but had no effect on phosphoPDE3Aser^{312}. In comparison thrombin (0.1 U/ml) induced significantly less phosphorylation at ser^{428}, which peaked at 1 min before returning to basal at 2 minutes (Figure 4H), but also induced phosphorylation of ser^{312}. These data confirm that oxLDL and its associated oxidised phospholipids require the sequential ligation and activation of CD36, Src, Syk and PKC to activate PDE3A.

Dyslipidaemia is associated with platelet PGI_2 hyposensitivity in mice.

To demonstrate the functional importance of our observations on dyslipidaemia driven thrombosis, we examined platelet sensitivity to PGI_2 in mice fed a Western diet (45%). cAMP signaling, integrin $\alpha_{IIb}\beta_3$ activation and thrombosis were assessed in whole blood *ex vivo*, this allowed us to evaluate platelet function and thrombotic potential while avoiding any confounding effects of altered PGI_2 synthesis *in vivo* associated with dyslipidaemia[32]. Western diet significantly raised cholesterol levels (Suppl. Figure 8) and the presence of oxidised phospholipids in the plasma (Figure 5A). We then investigated the effect of dyslipidaemia on cAMP signaling using multiplexed phosphoflow cytometry to allow the examination of signaling under the physiological conditions of whole blood[24]. Platelets from high-fat fed WT animals produced significantly less phosphoVASP-ser^{157} when challenged with PGI_2 (100 nM) than normal chow WT mice(4.9±0.4 fold versus 6.2±0.2 fold increase over basal; $p<0.05$) (Figure 5B). The deletion of CD36 protected cAMP signaling in dyslipidaemic blood with phosphoVASP-ser^{157} remaining at control levels (Figure 5B). In parallel experiments, blood was stimulated with CRP-XL (10 μg/ml), in the presence and absence of PGI_2 (100 nM), and $\alpha_{IIb}\beta_3$ activation measured. In normal chow WT blood, PGI_2 caused 75.7±3.9% inhibition of integrin activation ($p<0.05$ compared to absence of PGI_2), which was blunted in high-fat fed WT blood (43.1%±7.6 inhibition, $p<0.05$, compared to normal chow) Figure 5Ci). Conversely, in $CD36^{-/-}$ blood, PGI_2 induced inhibition of integrin activation was not significantly different in normal chow and high-fat fed conditions (66.5±8% and 79.3±6.5% respectively) (Figure 5Ci and Cii).

When we assessed ex vivo thrombosis under flow normal chow WT blood formed small thrombi on immobilised collagen in a time dependent manner, which was abolished by PGI_2 (20 nM) (Figure 5Di). High-fat fed WT blood showed an accelerated thrombotic response with increased surface area (11±3.6% compared to 16.2±4.3% at 2 mins). In addition, dyslipidaemia induced significant hyposensitivity to PGI_2, with the prostanoid causing 31.7±10.7% inhibition compared 61.6±5.6% with normal chow ($p<0.05$; 2 minutes) (Figure 5ii and iii). In contrast, the accelerated platelet deposition on collagen and platelet hyposensitivity to PGI_2 was not detected in $CD36^{-/-}$ high-fat fed blood (Figure 5D). We repeated the experiments with 8-CPT-6-Phe-cAMP, as if PDE3A activation was responsible for the increased thrombotic potential associated with reduced sensitivity to PGI_2, then CPT-6-Phe-cAMP mediated inhibition of thrombosis would be unaffected by dyslipidaemia. The cAMP analogue caused a similar degree of inhibition of thrombosis in all genotypes, but critically, remained unaffected in the context of dyslipidaemia (WT-normal chow, 65.6±11.2%; WT-Western diet, 62.3± 7.7%; $CD36^{-/-}$-normal chow, 70.4±2.0%; $CD36^{-/-}$-Western diet, 62.3±5% inhibition) (Suppl. figure 9). Here we show a physiological role for

platelet CD36 in dyslipidaemia, where it drives a phenotype of platelet hyperactivity through the blockade of cAMP mediated inhibition.

OxLDL potentiation of thrombosis *in vivo* is prevented by inhibition of PDE3A.

To examine the role of oxLDL in thrombosis *in vivo* we used intravital microscopy following ferric chloride–induced carotid artery injury. Tail-vein injections of oxLDL (2.5mg/kg^{-1} bodyweight)[33,34] into WT mice accelerated post-injury thrombotic response at all time points compared to control PBS injection (Figures 6A-C; suppl. videos 1 and 2). Next animals were pretreated with milrinone to explore in principle whether PDE3A inhibition might diminish prothrombotic effects of oxLDL. Consistent with previous studies, modulation of PDE3A activity reduced murine thrombosis (Figure 6A-C)[23]. Importantly, the presence of milrinone (10 μmol/L) significantly reduced the ability of oxLDL to promote thrombosis at all time points post injury ($p<0.05$), (supple. video 3) suggesting the heightened thrombotic response in the presence of oxLDL could be related, at least in part, to changes in PDE3A activity.

DISCUSSION

The presence of oxidised lipid epitopes, including oxLDL, is thought to promote platelet hyperactivity in subjects with obesity, CAD and stroke[5,6,35]. It is established that oxidative modifications are a hallmark of dyslipidemia and these stimulate platelet activation directly through a number of distinct receptors[6,8,13]. Interestingly, platelets from patients with CAD and dyslipidemia show a reduced sensitivity to the inhibitory effects of PGI_2. These observations coupled to pharmacological trials indicating that suppression of endothelial PGI_2 synthesis increased rate of atherothrombotic events[36–39] suggest that platelet sensitivity to PGI_2 could play an undefined role in the development of atherothrombotic events. Hence the aim of this study was to investigate whether oxLDL may promote unwanted platelet activation through the modulation of platelet sensitivity to PGI_2. Using a combination of pharmacological and genetic approaches we show that oxidative lipid stress modulates platelet cAMP signaling leading to increased platelet activation. Our key findings include (i) oxLDL and oxidised phospholipids decrease platelet sensitivity to PGI_2, which is coupled to reduced platelet accumulation of cAMP and PKA mediated signaling, (ii) PGI_2 hyposensitivity likely occurs via sustained activation of the cAMP hydrolysing enzyme PDE3A in response to oxLDL, (iii) the activation of PDE3A by oxLDL requires ligation of CD36, and (iv) that dyslipidaemia induces platelet hyposensitivity to PGI_2 in a CD36-dependent manner.

In the first instance we used three increasingly physiological systems to show that exposure of platelets to oxLDL opposes the inhibitory effects of PGI_2. In contrast, oxLDL failed to affect platelet inhibition by 8-CPT-6-Phe-cAMP, a PDE-resistant cAMP analogue, demonstrating firstly that the PKA signalling was intact, and secondly, that the effects of the oxidised lipoprotein may regulate cAMP availability. Exploration of the underlying mechanisms demonstrated that OxLDL prevented the accumulation of cAMP in response to both PGI_2 and forskolin. Forskolin increases cAMP in a receptor-independent manner, thereby provides evidence that oxLDL did not affect the interaction of PGI_2 with the IP receptor or target adenylyl cyclases. This is consistent with previous studies demonstrating that reduced platelet sensitivity to PGI_2 in patients with hypercholesterolaemia was independent of any changes in cAMP synthesis by adenylyl cyclase[36]. It was therefore possible that oxLDL could either prevent the synthesis of cAMP or accelerate its break down. We further found that oxLDL failed to modulate cAMP concentrations in the presence of the PDE3 inhibitor milrinone, but not the PDE2 inhibitor EHNA, suggesting that cAMP hydrolysis by PDE3A was the potential mediator of PGI_2 hyposensitivity. A role for PDE3A was confirmed using immunoprecipitation experiments showing that both oxLDL and $oxPC_{CD36}$ accelerated the hydrolytic activity of PDE3A in both human and murine platelets through ligation of CD36. The activation of PDE3A downstream of CD36 required the activation of Src family kinases, Syk and PKC. This provides further evidence that CD36-SFK-Syk represents a multiprotein complex that transduces extracellular oxidative lipid stress to the intracellular signalling machinery of the platelet. Interestingly, haemostatic agonists such as thrombin and collagen also activate PDE3A through a PKC-dependent mechanism[31]. These agonists are proposed to cause a rapid attenuation of cAMP signalling at sites of vascular injury to promote platelet-mediated haemostasis. However, in contrast to the rapid and short-lived activation of PDE3A activity by thrombin and collagen, oxLDL induced a sustained PDE3A response for up to 60 minutes (longest time tested). This was linked to a different activatory phosphorylation pattern of PDE3A by oxLDL and could suggest a distinct mechanism of activation induced by short-lived haemostatic agonists from that of oxLDL. Given the sustained activation of platelet PDE3A in the presence of oxidative lipid stress, it is attractive to speculate that PDE3A may be partially activated in dyslipidaemic disease states and thereby reduce the threshold for platelet activation by diminution of cAMP. Indeed, gain of function mutations of PDE3 are associated with stroke, underlining its role in vascular pathology[40]. This concept is also supported by the observations that inhibtion of PDE3A by cilostazol can have beneficial anti-thrombotic effects in high risk groups characterised by a prothrombotic phenotype [41–43].

The pathophysiological consequences of platelet hyposensitivity to PGI_2 and the potential importance of CD36 was explored in a murine model of high-fat feeding induced dyslipidaemia. Interestingly, we found that even mild dyslipidaemia was characterised by the presence of oxidised lipid epitopes in the plasma, which was unaffected by the absence of CD36. Whole blood phospho-flow cytometry was used to measure platelet phosphoVASP, as a marker of cAMP signalling, without the need for cell isolation. This demonstrated that mild dyslipidaemia was accompanied by reduced cAMP signalling. The functional importance of this blunted cAMP signalling response manifested as diminished platelet sensitivity to the inhibitory effects of PGI_2 on integrin activation measured by flow cytometry and *ex vivo* thrombosis. The assessment of thrombosis *ex vivo* was important to demonstrate that hyposensitivity of platelets to PGI_2 was a primary platelet defect rather than a response to a dysfunctional endothelium, where altered PGI_2 production has been observed in models of dyslipidaemia[32]. To support our hypothesis that hyposensitivity to PGI_2 was linked to PDE3A activity, we showed that cAMP signalling in dyslipidaemia was normal if a PDE-resistant cAMP (8-CPT-6-Phe-cAMP) was used, again confirming that PKA signalling downstream of cAMP was functional. Critically, genetic ablation of CD36, protected animals from the loss of PGI_2 sensitivity and restored PKA signalling. Infusions of oxLDL into wild type mice caused a robust potentiation of thrombosis induced by ferric chloride. However, mice were protected from the prothrombotic effects of oxLDL *in vivo* when PDE3A was pharmacologically inhibited. Using this approach milrinone did not target only platelets and could therefore have effects on other PDE3A expressing cells. However, the data are proof of principle that the pro-thrombotic effects of oxLDL *in vivo*, at least in part, may be prevented by therapeutic strategies based on enhancing or preserving cAMP signalling events in platelets. This element of the work requires further studies focussing on strategies for the specific targeting of PDE3A, and potentially PDE2, in platelets.

Together, our *ex vivo* and *in vitro* data suggests a previously unrecognised mechanism contributing to platelet hyperactivity, whereby the ligation of CD36 by oxidised lipids modulates cAMP signalling through activation of PDE3A activation leading to PGI_2 hyposensitivity. This data may constitute a link to the observed PGI_2 hyposensitivity in dyslipidaemic high-risk populations and indicate a novel therapeutic strategy to target atherothrombotic risk in certain patient groups. Remarkably, current antiplatelet therapy exclusively targets platelet activatory pathways including cyclooxygenases (Aspirin), P2Y12 (Thienopyridines, non-Thienopyridines) or $\alpha_{IIb}\beta_3$ (Tirofiban; Eptifibatide) while platelet inhibitory pathways remain untargeted. Therefore, high-risk populations might remain at increased atherothrombotic risk despite optimal available pharmacological therapy and impaired platelet inhibition might contribute to the residual cardiovascular risk.

References

1. Mitchell JA, Ali F, Bailey L, Moreno L, Harrington LS. Role of nitric oxide and prostacyclin as vasoactive hormones released by the endothelium. Exp Physiol. 2008;93(1):141–147.
2. Jackson SP. Arterial thrombosis--insidious, unpredictable and deadly. Nat Med. 2011;17(11):1423–1436.
3. Davì G, Romano M, Mezzetti A, et al. Increased levels of soluble P-selectin in hypercholesterolemic patients. Circulation. 1998;97(10):953–957.
4. Carvalho AC, Colman RW, Lees RS. Platelet function in hyperlipoproteinemia. N Engl J Med. 1974;290(8):434–438.
5. Colas R, Sassolas A, Guichardant M, et al. LDL from obese patients with the metabolic syndrome show increased lipid peroxidation and activate platelets. Diabetogia. 2011;54(11):2931–2940.
6. Chan H-CC, Ke L-YY, Chu C-SS, et al. Highly electronegative LDL from patients with {ST-elevation} myocardial infarction triggers platelet activation and aggregation. Blood. 2013;122(22):3632–3641.
7. Ardlie NG, Selley ML, Simons LA. Platelet activation by oxidatively modified low density lipoproteins. Atherosclerosis.1989;76(2–3):117–124.
8. Chen R, Chen X, Salomon RG, M, McIntyre T. Platelet activation by low concentrations of intact oxidized LDL particles involves the PAF receptor. Arterioscler. Thromb Vasc Biol. 2009;29(3):363–371.
9. Naseem KM, Goodall AH, Bruckdorfer KR. Differential effects of native and oxidatively modified low-density lipoproteins on platelet function. Platelets. 1997;8(2–3):163–173.
10. van Willigen G, Gorter G, Akkerman JW. LDLs increase the exposure of fibrinogen binding sites on platelets and secretion of dense granules. Arterioscler Thomb. 1994;14(1):41–46.
11. Podrez EA, Byzova T V, Febbraio M, et al. Platelet CD36 links hyperlipidemia, oxidant stress and a prothrombotic phenotype. Nat Med. 2007;13(9):1086–1095.
12. Korporaal S, Eck M, Adelmeijer J, et al. Platelet Activation by Oxidized Low Density Lipoprotein Is Mediated by Cd36 and Scavenger {Receptor-A}. Arterioscler. Thromb Vasc Biol. 2007;27(11):2476–2483.
13. Chen K, Febbraio M, Li W, Silverstein RL. A Specific CD36-Dependent Signaling Pathway Is Required for Platelet Activation by Oxidized Low-Density Lipoprotein. Circ Res. 2008;102(12):1512–1519.
14. Wraith KS, Magwenzi S, Aburima A, et al. Oxidized low-density lipoproteins induce rapid platelet activation and shape change through tyrosine kinase and Rho kinase-signaling pathways. Blood. 2013;122(4):580–589.
15. Biswas S, Zimman A, Gao D, Byzova T V, Podrez EA. TLR2 Plays a Key Role in Platelet Hyperreactivity and Accelerated Thrombosis Associated With Hyperlipidemia. Circ Res. 2017;121(8):951–962.
16. Chen K, Li W, Major J, et al. Vav guanine nucleotide exchange factors link hyperlipidemia and a prothrombotic state. Blood. 2011;117(21):5744–5750.
17. Magwenzi S, Woodward C, Wraith KS, et al. Oxidized LDL activates blood platelets through CD36/NOX2-mediated inhibition of the cGMP/protein kinase G signaling cascade. Blood. 2015;125(17):2693–2703.
18. Yang M, Cooley BC, Li W, et al. Platelet CD36 promotes thrombosis by activating redox sensor ERK5 in hyperlipidemic conditions. Blood. 2017;129(21):2917–2927.
19. Yang M, Kholmukhamedov A, Schulte ML, et al. Platelet CD36 signaling through ERK5 promotes caspase-dependent procoagulant activity and fibrin deposition in vivo. Blood Adv. 2018;2(21):2848–2861.
20. Raslan Z, Naseem KM. The control of blood platelets by cAMP signalling. Biochem. J Trans. 2014;42(2):289–294.
21. Beck F, Geiger J, Gambaryan S, et al. Time-resolved characterization of cAMP/PKA-dependent signaling reveals that platelet inhibition is a concerted process involving multiple signaling pathways. 2014;123(5):e1–e10.
22. Beca S, Ahmad F, Shen W, et al. Phosphodiesterase type 3A regulates basal myocardial contractility through interacting with sarcoplasmic reticulum calcium {ATPase} type 2a signaling complexes in mouse heart. Circ Res. 2013;112(2):289–297.
23. Sim DS, Glenn M-S, Furie BC, Furie B, Flaumenhaft R. Initial accumulation of platelets during arterial thrombus formation in vivo is inhibited by elevation of basal cAMP levels. Blood. 2004;103(6):2127–2134.
24. Spurgeon BE, Aburima A, Oberprieler NG, Taskén K, Naseem KM. Multiplexed phosphospecific flow cytometry enables large-scale signaling profiling and drug screening in blood platelets. J Thromb Haemost. 2014;12(10):1733–1743.
25. Haslam RJ, Dickinson NT, Jang EK. Cyclic nucleotides and phosphodiesterases in platelets. Thromb Haemost. 1999;82(2):412–423.
26. Conti M, Beavo J. Biochemistry and Physiology of Cyclic Nucleotide Phosphodiesterases: Essential Components in Cyclic Nucleotide Signaling. Annu Rev Biochem. 2007;76(1):481–511.
27. Butt E, Abel K, Krieger M, et al. cAMP- and cGMP-dependent protein kinase phosphorylation sites of the focal

adhesion vasodilator-stimulated phosphoprotein (VASP) in vitro and in intact human platelets. J Biol Chem. 1994;269(20):14509–14517.
28. Chen K, Febbraio M, Li W, Silverstein RL. A specific CD36-dependent signaling pathway is required for platelet activation by oxidized low-density lipoprotein. Circ Res. 2008;102(12):1512–1519.
29. Podrez E a, Byzova T V, Febbraio M, et al. Platelet CD36 links hyperlipidemia, oxidant stress and a prothrombotic phenotype. Nat Med. 2007;13(9):1086–1095.
30. Butt E, Abel K, Krieger M, Palm D, et al. cAMP-and cGMP-dependent protein kinase phosphorylation sites of the focal adhesion vasodilator-stimulated phosphoprotein (VASP) in vitro and in intact human platelets. J Biol Chem. 1994;269(20):14509-14517.
31. Hunter RW, Carol M, Hers I. Protein Kinase C-mediated Phosphorylation and Activation of PDE3A Regulate {cAMP} Levels in Human Platelets. J Biol Chem. 2009;284(18):12339–12348.
32. Csányi G, Gajda M, Magdalena F-Z, et al. Functional alterations in endothelial NO, PGI_2 and EDHF pathways in aorta in {ApoE/LDLR-/- mice. Prostaglandins Other Lipid Mediat. 2012;98(3–4):107–115.
33. Nakano A, Kawashima H, Miyake Y, et al. 123I–Labeled oxLDL Is Widely Distributed Throughout the Whole Body in Mice. Nucl Med Mol Imaging. 2018;52(2):144-153.
34. Badrnya S, Schrottmaier WC, Kral JB, et al. Platelets mediate oxidized low-density lipoprotein-induced monocyte extravasation and foam cell formation. Arterioscler. Thromb Vasc Biol. 2014;34(3):571–580.
35. Shen M-YY, Chen F-YY, Hsu J-FF, et al. Plasma L5 levels are elevated in ischemic stroke patients and enhance platelet aggregation. Blood. 2016;127(10):1336–1345.
36. Colli S, Lombroso M, Maderna P, Tremoli E, Nicosia S. Effects of PGI2 on platelet aggregation and adenylate cyclase activity in human type {IIa} hypercholesterolemia. Biochem Pharmacol. 1983;32(13):1989–1993.
37. Sinzinger H, Schernthaner G, Kaliman J. Sensitivity of platelets to prostaglandins in cornary heart disease and angina pectoris. Prostaglandins. 1981;22(5):773–781.
38. Mehta J, Mehta P, Conti CR. Platelet function studies in coronary heart disease. {IX.} Increased platelet prostaglandin generation and abnormal platelet sensitivity to prostacyclin and endoperoxide analog in angina pectoris. Am J Cardiol. 1980;46(6):943–947.
39. Furberg CD, Psaty BM, A FG. Parecoxib, valdecoxib, and cardiovascular risk. Circulation. 2005;111(3):249.
40. Malik R, Chauhan G, Traylor M, et al. Multiancestry genome-wide association study of 520,000 subjects identifies 32 loci associated with stroke and stroke subtypes. Nat Genet. 2018;50(4):524–537.
41. Araki S, Matsuno H, Haneda M, et al. Cilostazol attenuates spontaneous microaggregation of platelets in type 2 diabetic patients with insufficient platelet response to aspirin. Diabetes Care. 2013;36(7):e92-3.
42. Park KW, Kang S-H, Park JJ, et al. Adjunctive Cilostazol Versus Double-Dose Clopidogrel After Drug-Eluting Stent Implantation. JACC Cardiovasc Interv. 2013;6(9):932–942.
43. Angiolillo DJ, Capranzano P, Ferreiro JL, et al. Impact of adjunctive cilostazol therapy on platelet function profiles in patients with and without diabetes mellitus on aspirin and clopidogrel therapy. Thromb Haemost. 2011;106(2):253–262.

Figure 1: OxLDL induces PGI_2 hyposensitivity in platelets.
(A) Washed human platelets (2.5 x 10^8/ml) were treated alone or with nLDL or oxLDL (50µg/ml) for 2 minutes followed by a 1 minute incubation with PGI_2 (20nM). Thrombin(0.05U/ml)-stimulated aggregation was then measured under constant stirring (1000 rpm) at 37°C for 4 minutes. In some cases, platelets were incubated with either thrombin, nLDL or oxLDL alone for 4minutes. (i) Representative aggregation traces. (ii) Percentage

aggregation is presented by mean ± SEM (n= 5, **p< 0.01 compared to platelets treated with thrombin and PGI_2, Mann-Whitney U Test). **(B)** Whole blood was treated as in (A) and activated with PAR-1 peptide (10μM) for 5 minutes followed by fixation. P-selectin expression was assessed by flow cytometry. Representative data of 3 independent experiments. (i) Data is presented as heatmap of fold-change MFI. (ii) representative histograms. **(C)** Human whole blood was incubated with PGI_2 (20nM) for 1 minute alone or with nLDL or oxLDL (50μg/ml) for 10 minutes. Blood was perfused over collagen-coated biochips for 2 minutes at arterial shear $1000s^{-1}$ and images of adherent platelets were taken by fluorescence microscopy. (i) The surface coverage (%) is presented as mean±SEM (n=3)($p<0.05$, Mann-Whitney U Test). (ii) Representative fluorescence microscopy images are shown. **(D)** Whole blood was incubated with nLDL or oxLDL (50μg/ml) for 10 minutes and then perfused over collagen-coated surfaces for 2 minutes at arterial shear $1000s^{-1}$. Thrombi were post-stained with anti-oxPC antibody and images were taken by fluorescence microscopy. (i) Representative of images of 3 independent experiments. Stained with $DIOC_6$ (top panel) or anti-oxPC (bottom panel) (ii) The surface coverage is presented as mean ± SEM (n=4, *p< 0.05, Mann-Whitney U Test). (iii) Fluorescence (red Channel) is presented as mean ± SEM (n=4, *p< 0.05, Mann-Whitney U Test).

Figure 2: OxLDL modulates cAMP signalling in response to PGI_2.
(A) Washed human platelets ($2x10^8$/ml) incubated with apyrase, indomethacin and EGTA were treated alone or with nLDL or oxLDL (50μg/ml) for 2 minutes followed by a 1 minute PGI_2 (50nM) incubation. Platelets were lysed and intracellular cAMP concentrations were measured by enzyme immunoassay. (i) Intracellular cAMP levels presented as mean ± SEM (N=3, *p<0.05, Mann-Whitney U Test). (ii) Platelets treated as described under (A) in the presence EHNA (20μM). Intracellular cAMP levels presented as mean ± SEM (N=3, *p<0.05, Mann-Whitney U Test) (iii) Platelets treated as described under (A) in the presence of Milrinone (10μM). Intracellular cAMP levels presented as mean ± SEM (N=3, *p<0.05, Mann-Whitney U Test). **(B)** Washed human platelets ($2x10^8$/ml) incubated alone or with oxLDL (50μg/ml) for 2 minutes followed by a 5 minute incubation with Forskolin (10μM). Lysed and measured as described under (A). Intracellular cAMP concentrations presented as mean ± SEM (N=3, *p< 0.05, Mann-Whitney U Test). **(C)** Washed human platelets ($5x10^8$/ml) treated as described under (A), lysed in Laemmli buffer, separated by SDS-PAGE and immunoblotted with anti-phosphoPKA substrate, anti-phosphoVASPser^{157} and anti-β tubulin. (i) Representative blot of 3 independent experiments. (ii) Densitometry of the representative highlighted band (red) (*p<0.05, Mann-Whitney U Test) **(D)** Washed human platelets were treated as described under A except, platelets were treated with 8-CPT-cAMP (50μM) for 5 minutes and then processed as in (C). (i) Representative blot of three independent experiments and (ii) Densitometry of the representative highlighted band (red).

Figure 3: OxLDL and $oxPC_{CD36}$ alter PGI_2 inhibitory signalling via CD36.
(A) Washed human platelets ($5x10^8$/ml) incubated with apyrase, indomethacin and EGTA were incubated with FA6-152 or IgG (1μg/ml) for 20minutes. Platelets were then incubated alone or with nLDL or oxLDL (50μg/ml) for 2 minutes and subsequently stimulated by PGI_2 (50nM) for 1 minute. Treated platelets were lysed in Laemmli buffer, separated by SDS-PAGE and immunoblotted with anti-phosphoVASPser^{157} or anti-β tubulin. (i) Representative blot of 3 independent experiments. (ii) Densitometry of pVASPser^{157} fold-change above basal mean ± SEM (n=3 *p<0.05, Mann-Whitney U Test). **(B)** as in (A) except platelets were probed for phosphoVASPser^{239}. **(C)** Platelets treated as in (A) alone or with $oxPC_{CD36}$ or PAPC (25μM) for 2 minutes followed by PGI_2 (50nM) for 1 minute. (i) Representative blot of 3 independent experiments and (ii) Densitometry of pVASPser^{157} fold-change above basal, mean ± SEM (n=3 *p<0.05, Mann-Whitney U Test). **(D)** Washed wild-type murine platelets ($2.5x10^8$/ml) were treated alone or with $oxPC_{CD36}$ or PAPC (10μM) for 2 minutes followed by a 1 minute incubation with PGI_2 (20nM). Thrombin(0.05U/ml)-stimulated aggregation was then measured under constant stirring (1000 rpm) at 37°C for 4 minutes. (i) Representative aggregation traces and (ii) data presented as percentage aggregation, mean ± SEM (n=3, $p<0.05$, Mann-Whitney U Test). **(E)** As described in (D) for $CD36^{-/-}$ platelets. Ns= not significant. **(F)** Washed murine WT or $CD36^{-/-}$ platelets ($2x10^8$/ml) were treated alone or with nLDL or oxLDL (50μg/ml) for 2 minutes followed by a 1 minute PGI_2 (50nM) incubation. Platelets were lysed and intracellular cAMP concentrations were measured by enzyme immunoassay. Intracellular cAMP levels presented as mean ± SEM (n=3, *p<0.05, Mann-Whitney U Test). **(G)** as in (A) except murine (i) WT and (ii) $CD36^{-/-}$ platelets were used. Representative blot of 3 independent experiments. pVASPser^{157} is presented as beta-tubulin corrected fold-change above basal ± SEM (N=3 *p < 0.05, Mann-Whitney U Test).

Figure 4: OxLDL and $oxPC_{CD36}$ induce sustained PDE3A activity in a CD36-dependent manner.
(A) Washed human platelets ($5x10^8$/ml) incubated with apyrase, indomethacin and EGTA were (i) incubated with nLDL (50μg/ml) or oxLDL (10-100μg/ml) for 2minutes or (ii) incubated with nLDL (50μg/ml) or oxLDL (50μg/ml) for up to 60 minutes. Platelets were lysed, PDE3A immunoprecipitated and enzyme activity was measured. Data is expressed as % activity above basal activity and presented as mean ± SEM ($p<0.05$; n=3, Kruskal-Wallis Test). **(B)** Washed human platelets ($5x10^8$/ml) were incubated with oxLDL (50μg/ml) for up to 60 minutes followed by PGI_2 (50nM) for 1 minute. Platelets were lysed and intracellular cAMP levels were determined by enzyme immunoassay.

Data is presented as mean ± SEM (* p<0.05; n=3, Kruskal-Wallis Test). **(C)** Washed human platelets ($5x10^8$/ml) were incubated with $oxPC_{CD36}$ or PAPC (25μM) for 2 minutes and activity of immunoprecipitated PDE3A measured. Data is expressed as % activity above basal activity and presented as mean ± SEM (p <0.05; n=3 Mann-Whitney U Test). **(D)** and in (C) except PDE3A activity was measured in WT and $CD36^{-/-}$ washed platelets (*p<0.05; n=3 Mann-Whitney U Test). **(E)** as in (A) except human platelets ($5x10^8$/ml) incubated with apyrase, indomethacin and EGTA were then treated with $oxPC_{CD36}$ or PAPC (25μM) for 2 minutes in the presence of absence of Dasatinib (10μM) or vehicle control (DMSO). PDE3A was immunoprecipitated and enzyme activity measured. Data is expressed as % activity above basal activity and presented as mean ± SEM (p <0.05; n=4 Mann-Whitney U Test). **(F)** as in (A) except platelet were treated with R406 (1μM) or vehicle control (DMSO). **(G)** as in (A) except platelets were treated with PKC inhibitors (RO31 10μM, BIM1 10μM), PMA (100nM), BAPTA (20μM) or vehicle control (DMSO). (n=3, * p < 0.05 compared to basal, Kruskal-Wallis Test). **(H)** Washed human platelets ($5x10^8$/ml) treated with apyrase, indomethacin and EGTA were incubated with or oxLDL (50μg/ml; 0-60minutes) or thrombin (0.1U/ml; 0-2minutes). Treated platelets were lysed in Laemmli buffer, separated by SDS-PAGE and immunoblotted with anti-phosphoPDE3Aser^{312}, phosphoPDE3Aser^{428} or anti-β tubulin. (i) Representative blot of 3 independent experiments (ii) densitometry for phosphoPDE3Aser^{428} is presented as fold-change above basal, mean ± SEM (n=3, *p<0.05, Kruskal-Wallis Test).

Figure 5: High-fat diet fed mice correlate increased plasma levels of oxidised phospholipids to reduced PGI_2 sensitivity via CD36.

(A) Representative dot blots of mouse plasma probed with anti-oxidised phospholipids (HRP-conjugated-E06) and total-IgG (HRP-conjugated anti-mouse). **(B)** Whole blood from normal chow and High-fat fed animals were treated with PGI_2 (100nM) for 1 minute. Blood was fixed, permeabilised and incubated with anti-pVASPser^{157} followed by secondary fluorescent-conjugate (Alexa 647) and analysed by flow-cytometry. (i) Representative heat map of fold increase in phosphoVASPser^{157}. Quantification is presented as fold-change of median fluorescence intensity above basal (n=4, *p<0.05, Mann-Whitney U Test). **(C)** Whole blood from normal chow and high-fat diet fed animals were treated with PGI_2 (100nM) for 1 minute followed by CRP (10μg/ml) for 5 minutes. Blood was fixed and JON/A positive cells were analysed by flow-cytometry. (i) Representative histograms. (ii) Data presented as percentage inhibition of JON/A binding, mean ± SEM (n=4 * p<0.05, Mann-Whitney U Test). **(D)** Whole blood incubated alone or with PGI_2 (2onM) for 1 minute was perfused at arterial shear $1000s^{-1}$ for 2 minutes over a collagen matrix (50μg/ml). Images of adherent platelets were taken by fluorescence microscopy. (i) surface coverage (%) presented as a function of time (ii) Representative images of arterial flow experiments, (iii) Data presented as inhibition of surface coverage (%), mean ± SEM (n=5; * p<0.05, Mann-Whitney U Test).

Figure 6: OxLDL induced thrombosis in vivo is prevent by inhibition of PDE3A.

Intravital microscopy was performed as described in "supplementary methods." (A) Representative fluorescence images of thrombi formed under different conditions are shown over the course of 40minutes after vascular injury. Black arrow shows the direction of blood flow. (B) Representative median integrated fluorescence signals of Rhodamine G obtained from an individual carotid thrombus under different conditions. (C) Quantified median integrated fluorescence signals from 10, 20, 30 and 40 minutes after vascular injury taken from 5 WT for each treatment. *p< 0.05; **p< 0.01, Kruskal-Wallis Test.

Figure 7: Proposed signalling pathway downstream of CD36 through which oxLDL activates PDE3A to suppress cAMP signalling.

OxLDL binds to CD36 to activate a tyrosine kinase signalling pathway that leads to a sustained activation of PDE3A. Under these conditions cAMP is maintained at low concentrations through hydrolysis to 5'AMP (solid red line) and the activation of PKA is diminished (dashed red line). Through disinhibition this pathway acts to reduce the threshold for platelet activation and promote thrombosis.

Figure 1

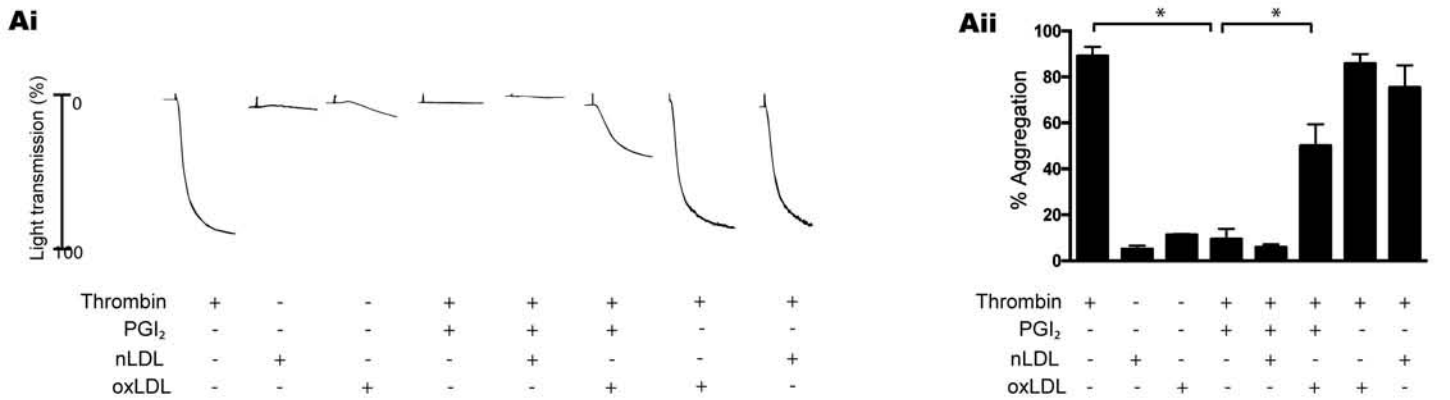
Ai
Light transmission (%)
0
100
Thrombin + - - + + + + +
PGI2 - - - + + + - -
nLDL - + - - + - - +
oxLDL - - + - - + + -
Aii
% Aggregation
100
80
60
40
20
0
*
*
Thrombin + - - + + + + +
PGI2 - - - + + + - -
nLDL - + - - + - - +
oxLDL - - + - - + + -

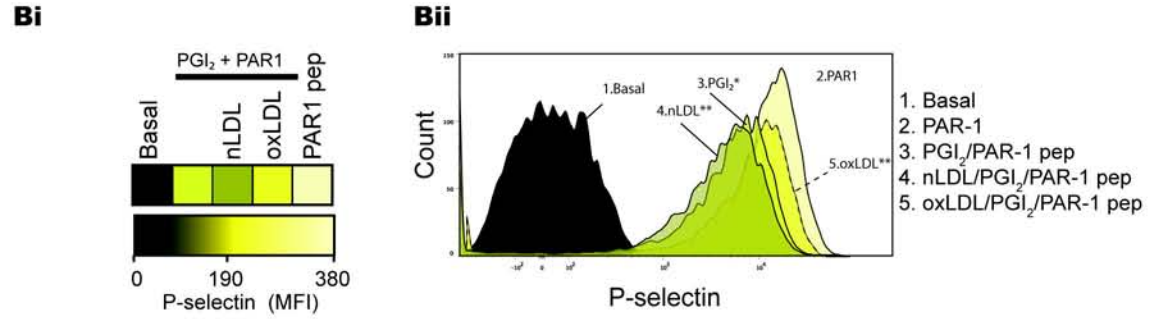
Bi
PGI2 + PAR1
Basal
nLDL
oxLDL
PAR1 pep
0
190
380
P-selectin (MFI)
Bii
Count
1.Basal
2.PAR1
3.PGI2*
4.nLDL**
5.oxLDL**
P-selectin
1. Basal
2. PAR-1
3. PGI2/PAR-1 pep
4. nLDL/PGI2/PAR-1 pep
5. oxLDL/PGI2/PAR-1 pep

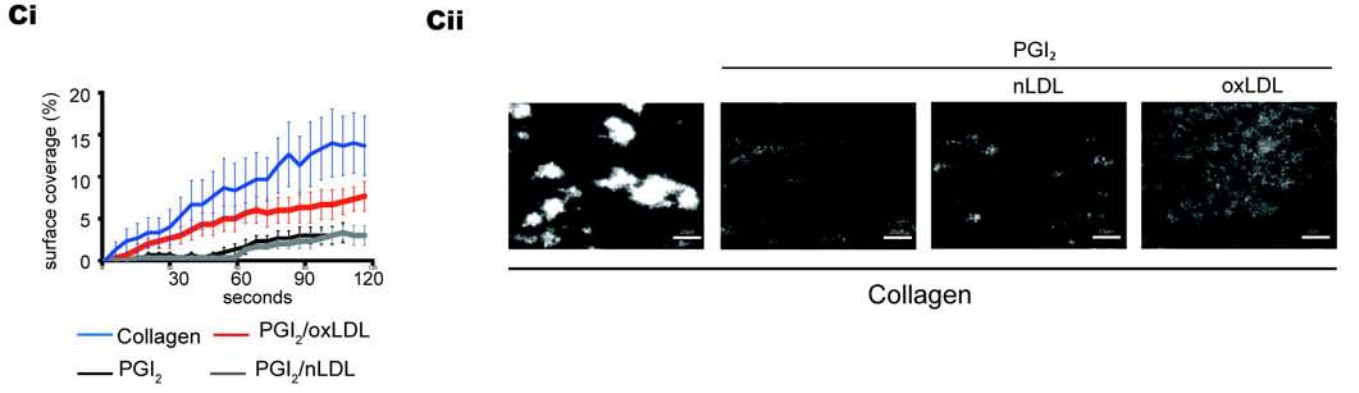
Ci
surface coverage (%)
20
15
10
5
0
30
60
90
120
seconds
Collagen
PGI2/oxLDL
PGI2
PGI2/nLDL
Cii
PGI2
nLDL
oxLDL
Collagen

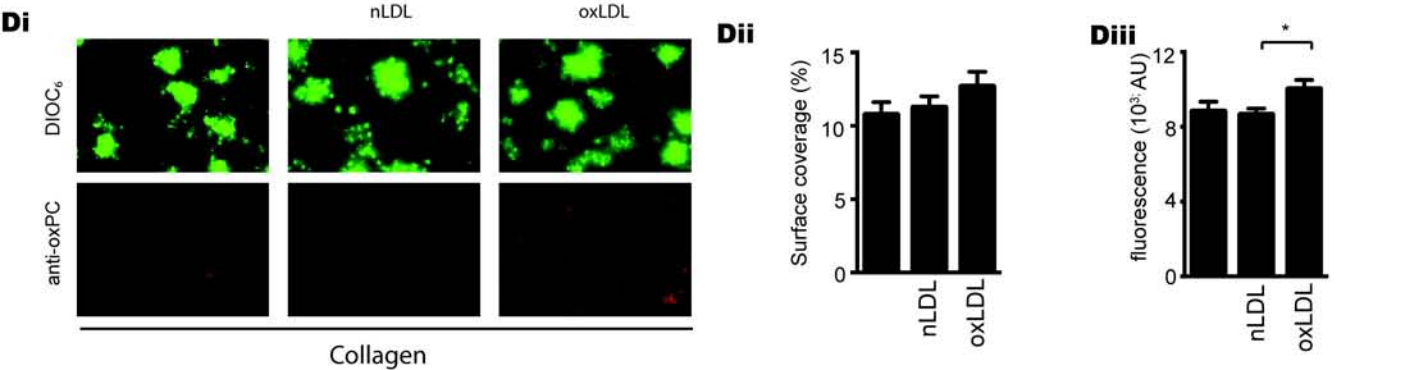
Di
nLDL
oxLDL
DIOC6
anti-oxPC
Collagen
Dii
Surface coverage (%)
15
10
5
0
nLDL
oxLDL
Diii
fluorescence (10³ AU)
12
8
4
0
*
nLDL
oxLDL

Figure 2

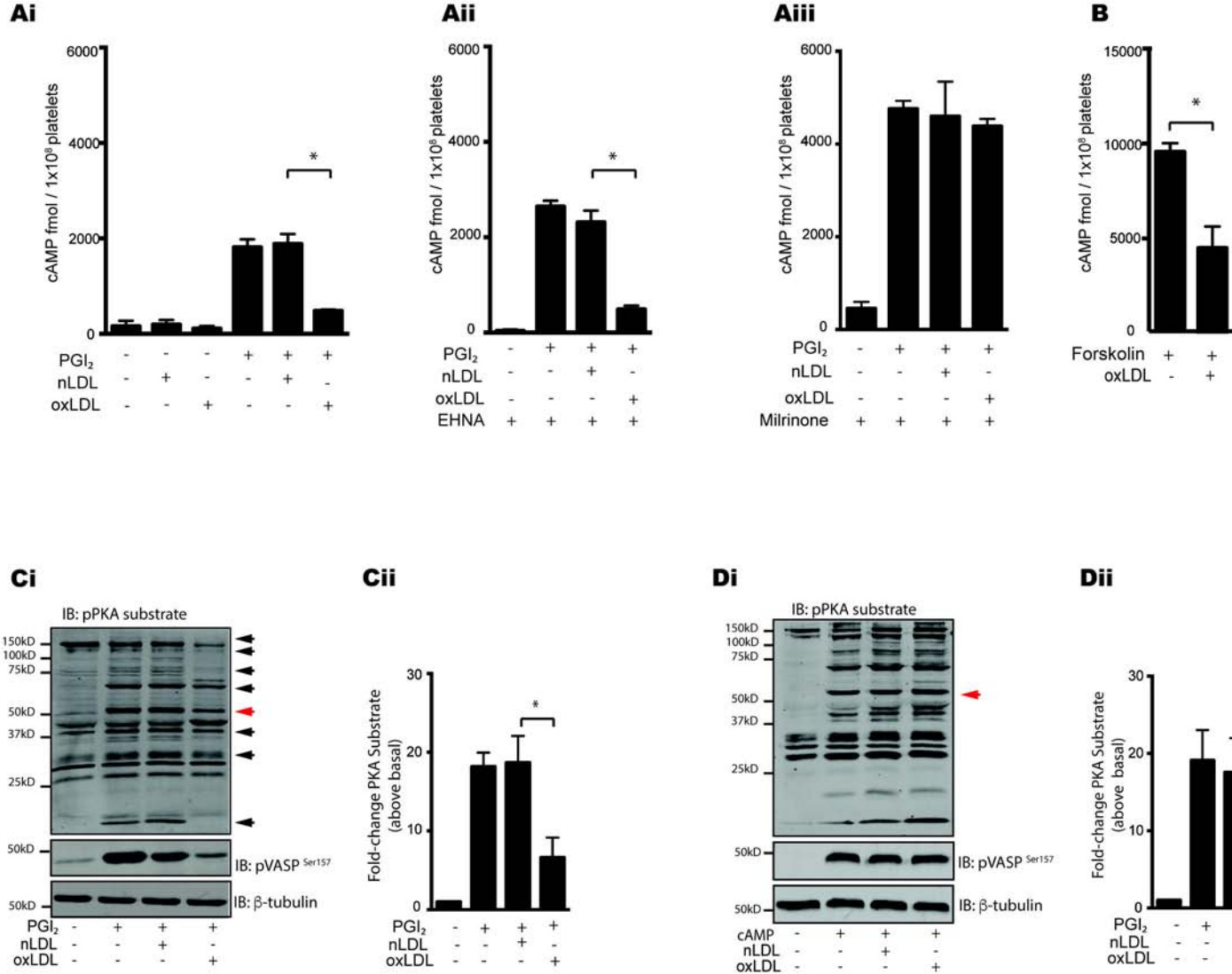
Ai
Aii
Aiii
B
cAMP fmol / 1x10⁸ platelets
6000
4000
2000
0
15000
10000
5000
*
PGI2
nLDL
oxLDL
EHNA
Milrinone
Forskolin
Ci
Cii
Di
Dii
IB: pPKA substrate
150kD
100kD
75kD
50kD
37kD
25kD
IB: pVASP Ser157
IB: β-tubulin
Fold-change PKA Substrate (above basal)
30
20
10
0
cAMP

Figure 3

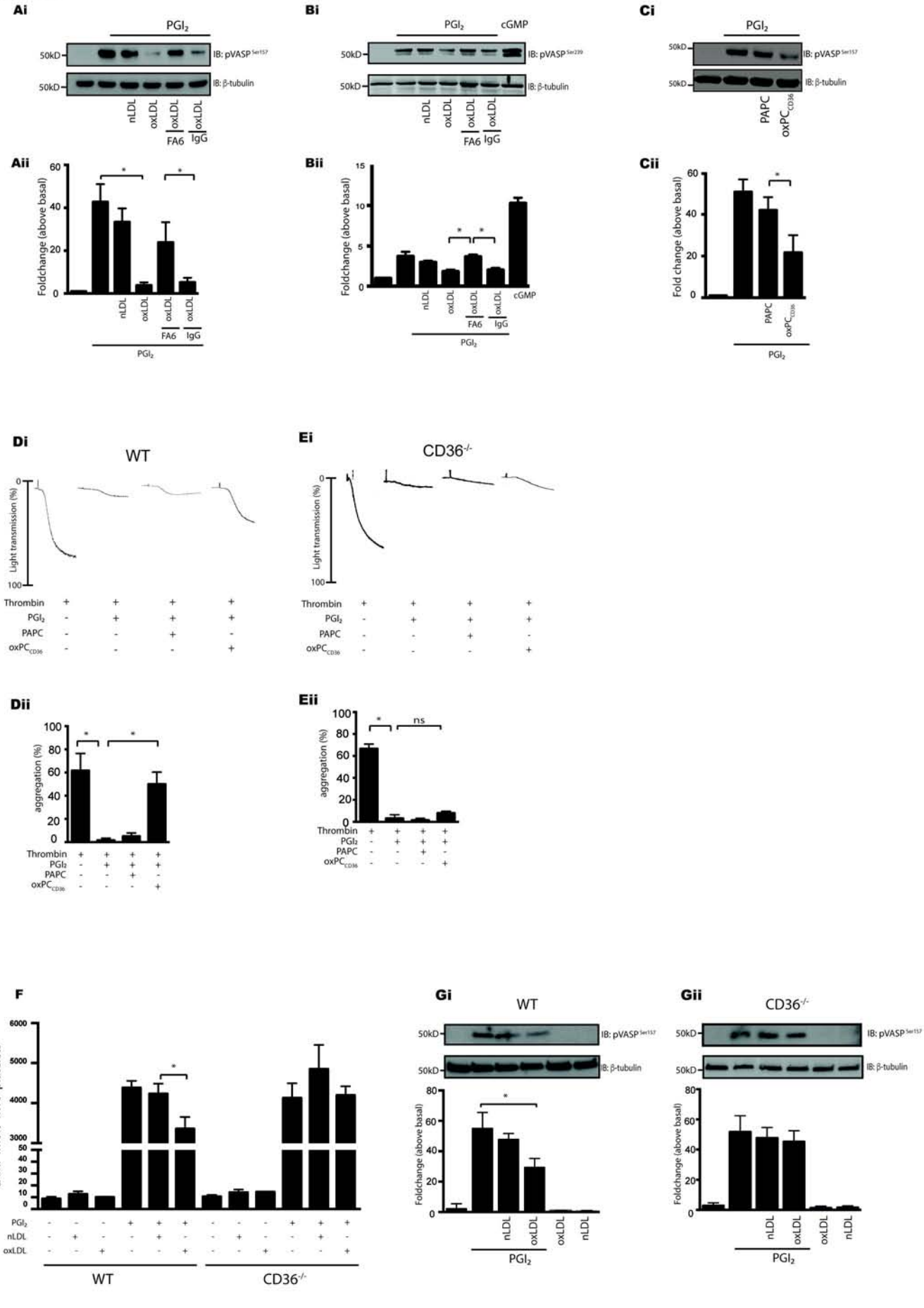
Ai
PGI2
50kD
IB: pVASP Ser157
IB: β-tubulin
nLDL
oxLDL
oxLDL FA6
oxLDL IgG
Bi
PGI2
cGMP
IB: pVASP Ser239
Ci
PGI2
IB: pVASP Ser157
IB: β-tubulin
PAPC
oxPC CD36
Aii
Foldchange (above basal)
PGI2
Bii
Foldchange (above basal)
cGMP
PGI2
Cii
Fold change (above basal)
PAPC
oxPC CD36
PGI2
Di
WT
Light transmission (%)
Thrombin
PGI2
PAPC
oxPC CD36
Ei
CD36-/-
Light transmission (%)
Thrombin
PGI2
PAPC
oxPC CD36
Dii
aggregation (%)
Thrombin
PGI2
PAPC
oxPC CD36
Eii
aggregation (%)
ns
Thrombin
PGI2
PAPC
oxPC CD36
F
cAMP fmol / 1x10^8 platelets
PGI2
nLDL
oxLDL
WT
CD36-/-
Gi
WT
IB: pVASP Ser157
IB: β-tubulin
Foldchange (above basal)
nLDL
oxLDL
oxLDL
nLDL
PGI2
Gii
CD36-/-
IB: pVASP Ser157
IB: β-tubulin
Foldchange (above basal)
nLDL
oxLDL
oxLDL
nLDL
PGI2

Figure 4

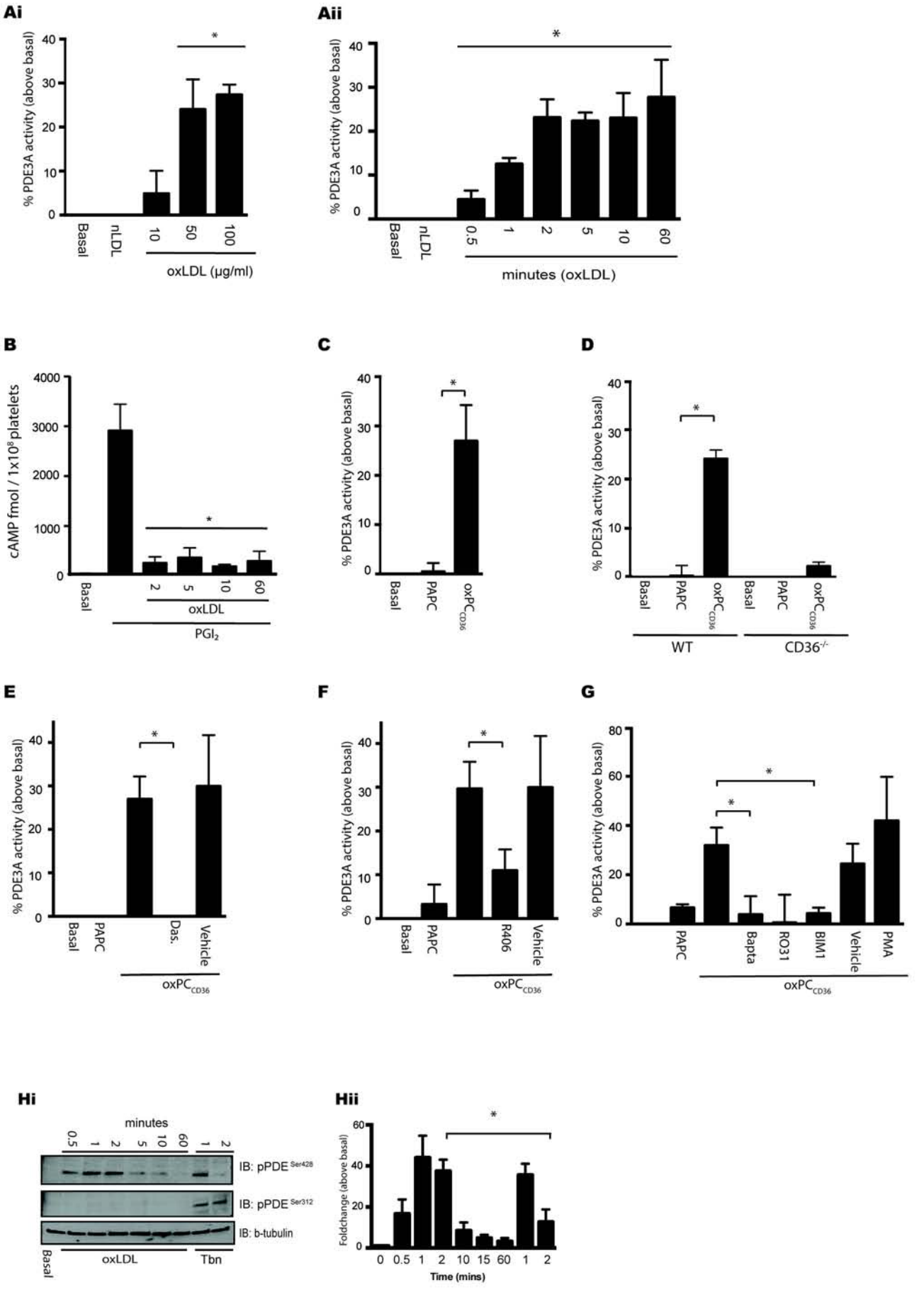
Ai
% PDE3A activity (above basal)
Basal
nLDL
10
50
100
oxLDL (µg/ml)
Aii
% PDE3A activity (above basal)
Basal
nLDL
0.5
1
2
5
10
60
minutes (oxLDL)
B
cAMP fmol / 1x10⁸ platelets
Basal
2
5
10
60
oxLDL
PGI2
C
% PDE3A activity (above basal)
Basal
PAPC
oxPCCD36
D
% PDE3A activity (above basal)
Basal
PAPC
oxPCCD36
WT
CD36-/-
E
% PDE3A activity (above basal)
Basal
PAPC
Das.
Vehicle
oxPCCD36
F
% PDE3A activity (above basal)
Basal
PAPC
R406
Vehicle
oxPCCD36
G
% PDE3A activity (above basal)
PAPC
Bapta
RO31
BIM1
Vehicle
PMA
oxPCCD36
Hi
minutes
0.5
1
2
5
10
60
1
2
IB: pPDE Ser428
IB: pPDE Ser312
IB: b-tubulin
Basal
oxLDL
Tbn
Hii
Foldchange (above basal)
0
0.5
1
2
10
15
60
1
2
Time (mins)

Figure 5

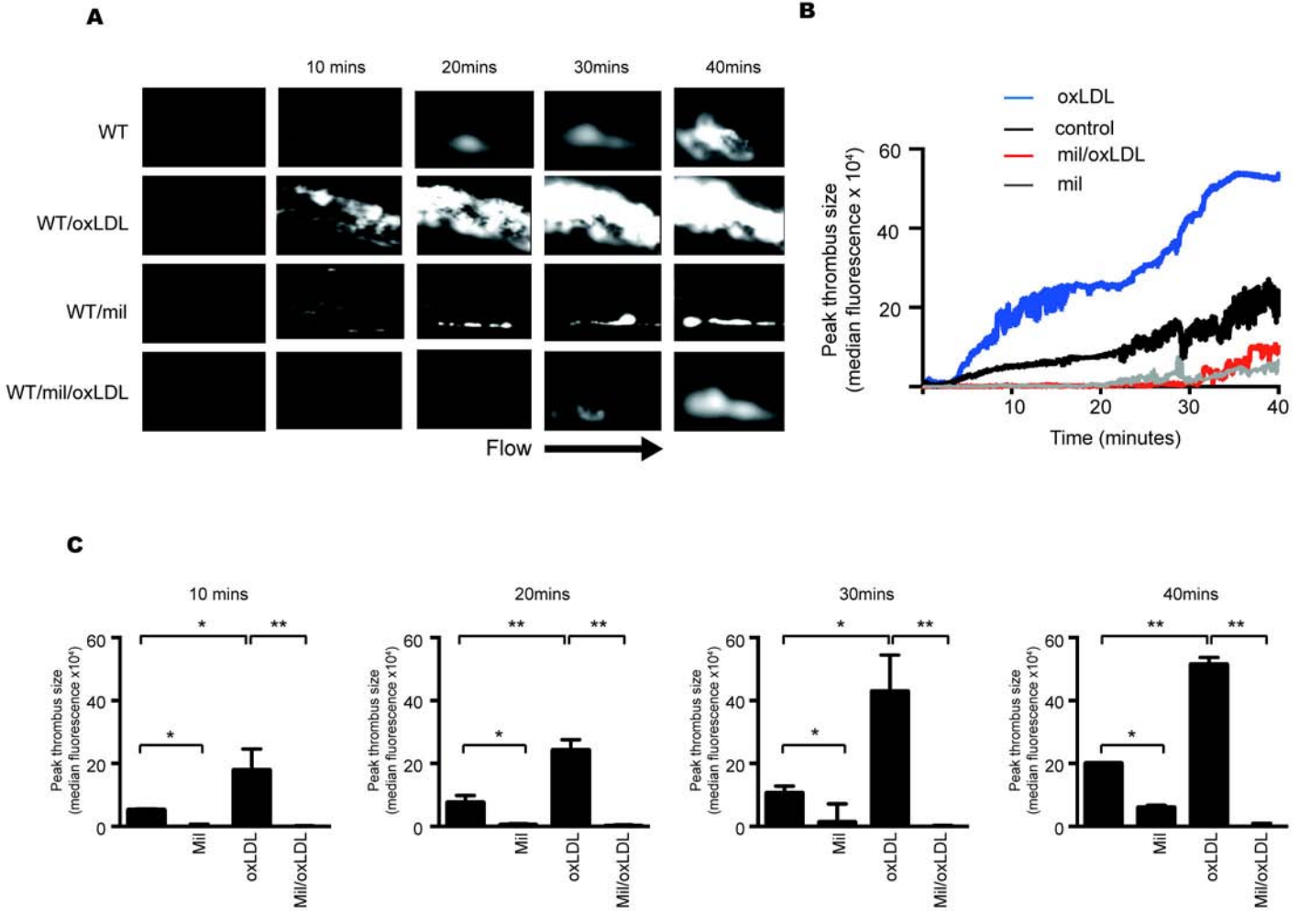
A
10 mins
20mins
30mins
40mins
WT
WT/oxLDL
WT/mil
WT/mil/oxLDL
Flow
B
oxLDL
control
mil/oxLDL
mil
Peak thrombus size (median fluorescence x 10⁴)
60
40
20
10
20
30
40
Time (minutes)
C
10 mins
20mins
30mins
40mins
Peak thrombus size (median fluorescence x10⁴)
60
40
20
0
*
**
Mil
oxLDL
Mil/oxLDL

Figure 6

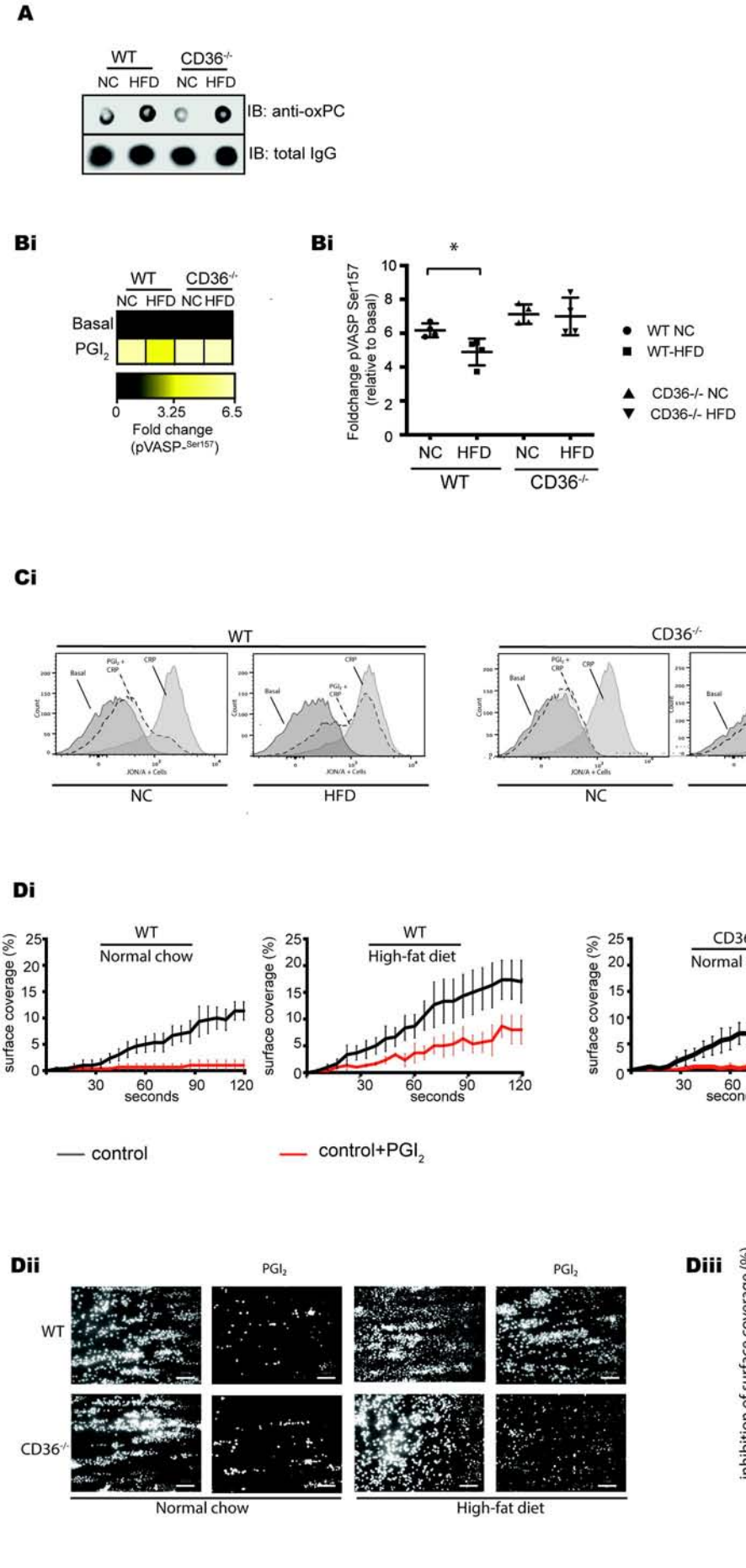
A
WT
CD36-/-
NC HFD NC HFD
IB: anti-oxPC
IB: total IgG
Bi
WT
CD36-/-
NC HFD NC HFD
Basal
PGI2
0
3.25
6.5
Fold change
(pVASP-Ser157)
Bi
*
Foldchange pVASP Ser157
(relative to basal)
10
8
6
4
2
0
NC HFD NC HFD
WT
CD36-/-
WT NC
WT-HFD
CD36-/- NC
CD36-/- HFD
Ci
WT
CD36-/-
Basal
PGI2 + CRP
CRP
Count
JON/A + Cells
NC
HFD
NC
HFD
Cii
*
100
50
0
% inhibition JON/A + Cells
NC HFD NC HFD
WT CD36-/-
PGI2
Di
WT
Normal chow
WT
High-fat diet
CD36-/-
Normal chow
CD36-/-
High-fat Diet
surface coverage (%)
25
20
15
10
5
0
30 60 90 120
seconds
control
control+PGI2
Dii
PGI2
PGI2
WT
CD36-/-
Normal chow
High-fat diet
Diii
*
inhibition of surface coverage (%)
100
80
60
40
20
0
NC HFD NC HFD
WT CD36-/-
PGI2

Figure 7

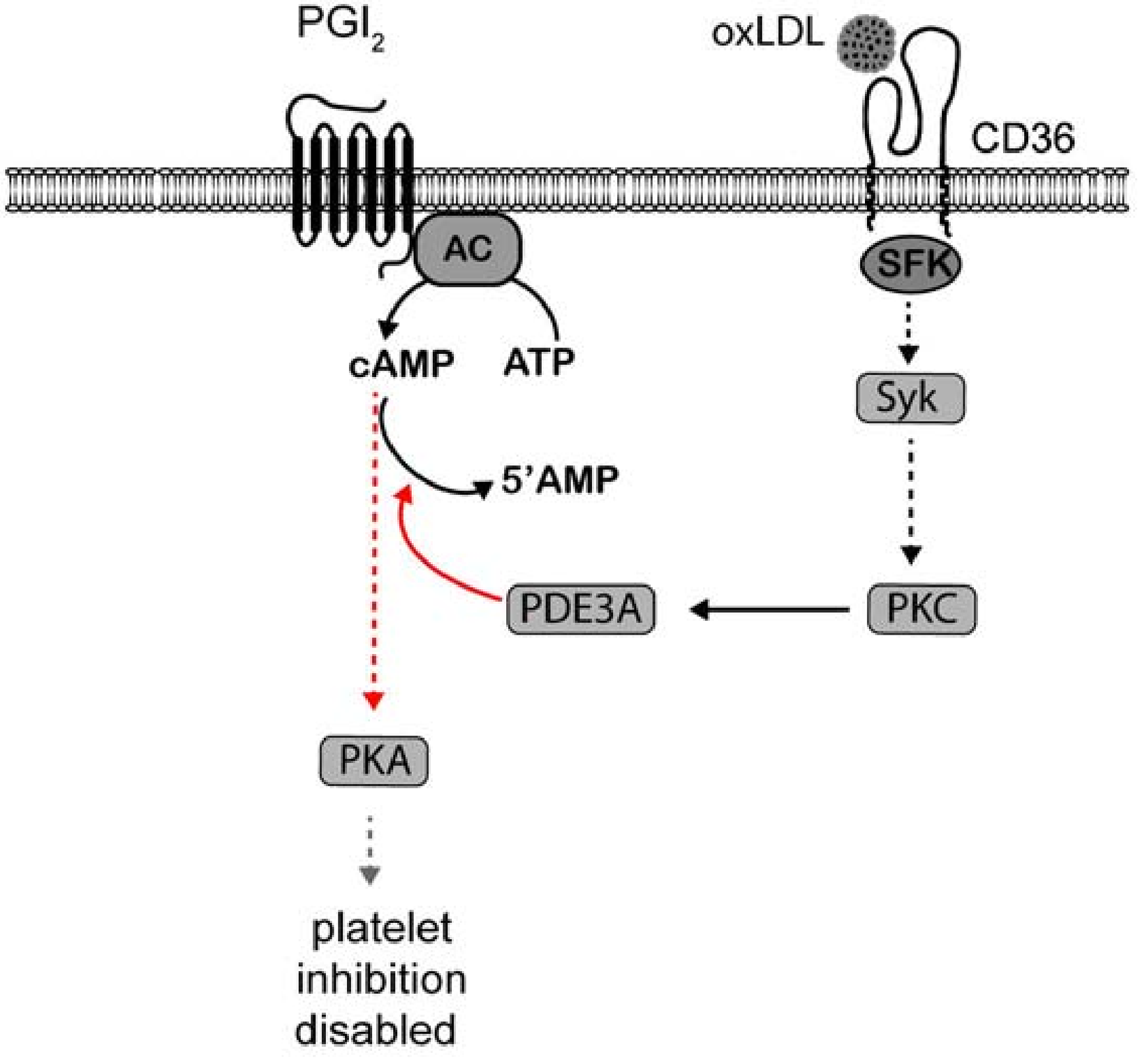
PGI2
oxLDL
CD36
AC
SFK
cAMP
ATP
Syk
5'AMP
PDE3A
PKC
PKA
platelet
inhibition
disabled

SUPPLEMENTARY METHODS.

Platelet preparation

Human washed platelets (WP) were isolated from blood taken from drug-free volunteers as previously described. [1] All Human work was approved by the Hull York Medical School Ethics Committee. Human blood was taken from drug-free volunteers by clean venepuncture using acid citrate dextrose (ACD; 29.9mM sodium citrate, 113.8mM glucose, 72.6mM sodium chloride and 2.9mM citric acid, pH 6.4) as anticoagulant. Platelet-rich plasma (PRP) was obtained by centrifugation of whole blood at 200g at 20°C for 20minutes. PRP was treated with citric acid (0.3M) and centrifuged at 800g for 12 minutes. The platelet pellet was then suspended in wash buffer (36mM citric acid, 10mM EDTA, 5mM glucose, 5mM KCl, 9mM NaCl) and spun once more at 800g for 12 minutes. Platelets were finally re-suspended at the indicated concentration in modified Tyrodes buffer (150mM NaCl, 5mM HEPES, 0.55mM NaH_2PO_4, 7mM $NaHCO_3$, 2.7mM KCl, 0.5mM $MgCl_2$, 5.6mM glucose, pH7.4).
Murine blood obtained by cardiac puncture was taken into PPACK by under terminal CO_2 narcosis. PRP was obtained by centrifugation of whole blood at 300*g* for 10min at room temperature. The PRP was then centrifuged at 1000*g* after addition of citric acid (0.3M) for 6minutes at room temperature. The pellet was resuspended in modified Tyrodes buffer, spun again at 1000g for 6minutes and then finally resuspended at the indicated concentration in modified Tyrodes buffer. When required for signalling experiments, platelets were incubated with ethylene-glycol-bis-tetraacetic acid (EGTA; 1mM), indomethacin (10μM) and apyrase (2U/ml) for 15 minutes before experimentation.

Platelet aggregation

WP (2.5×10^8 platelets/mL) were incubated with oxLDL/LDL (50μg/ml) at 37°C for 2 minutes followed PGI_2 (20nM) for 1 minute and then the addition of thrombin (0.05U/mL) or collagen (5μg/ml) and aggregation monitored under constant stirring for 4 minutes using a Chronolog Dual Channel Platelet Aggregometer.

Platelet flow assays

For the i*n vitro* thrombosis assay human whole blood was incubated with $DiOC_6$ (1μM) and treated with oxLDL/LDL (50μg/mL) in the presence and absence of PGI_2 (20nM). Assays were performed using Vena8 biochips (Cellix; Dublin, Ireland), coated with collagen (50μg/ml) for 12 hours, and blocked with BSA (10mg/mL) for 1hour. For *ex vivo* experiments murine blood was treated in the same manner except the addition of nLDL/oxLDL was omitted. Flow was performed for 2minutes at $1000s^{-1}$. Images of stably adhered platelets and thrombi were captured using fluorescence microscopy and analysed using ImageJ software. Data are presented as surface area coverage (%), since the software could not fully discriminate between single platelets and platelet aggregates. [2]

Flow cytometric analysis

Flow cytometry assays were performed with whole blood from either mice or human subjects. For human studies, whole blood was incubated with oxLDL/LDL (50μg/ml) at 37°C for 2 minutes, followed by PGI_2 (20nM) for 1 minute and the assay initiated by the addition of PAR-1 peptide (10μM). Flow cytometry was performed using a BD LSRFortessa and analysed for P-selectin expression. For murine studies blood was harvested and examined for phosphoVASP or JonA binding. For PhosphoVASP a phosphoflow cytometry approach was used. In brief, whole blood was incubated with PGI_2 (20nM) for 1 minute. Cells were then pelleted by centrifugation at 1000*g at* 4°C, for 10min, the supernatants removed and the remaining platelets permeabilised for 10 min with 0.1% Triton X-100 in phosphate buffered saline (PBS). Permeabilised platelets were pelleted (1000*g at* 4°C, for 10minutes) washed with PBS and incubated with phosphospecific antibodies (2μg/mL) on ice for 30 minutes. Platelets were washed with PBS and incubated with a secondary antibody labeled with AlexaFluor 647 (1μg/mL) on ice in the dark for 45 minutes. After washing with PBS, platelets were transferred to FACS tubes for flow cytometric analyses using a BD LSRFortessa. [3] For JON/A binding platelet were incubated with PGI_2 (100nM) for 1 minute followed by addition of CRP-XL (10μg/ml) for 5minutes. After fixation platelets were stained and processed using a BD LSRFortessa

Immunoblotting

Washed platelets (5×10^8 platelets/mL), incubated with apyrase (2U/mL), indomethacin (10μmol/L) and EGTA (1mmol/L), were treated with oxLDL/nLDL (50μg/ml for 15min) prior to the addition of PGI_2 (20nM) for 1 minute at 37°C before termination with Laemmli buffer. In some cases, platelets were incubated with the CD36 blocking antibody FA6-152 or IgG (1μg/mL), for 20min at 37°C prior to addition of oxLDL. Whole cell lysates were separated by SDS-PAGE and transferred to PVDF membranes. Membranes were blocked for 60minutes with 10% BSA or 5% milk dissolved in Tris-buffered-saline-Tween (0.1%)

(TBS-T) then incubated with anti-phosphoPKA substrate (1:1000), anti-phosphoVASP-ser^{239} (1:1000), anti-phosphoVASP-ser^{157} (1:1000), anti-pDE3Aser^{428} (1:250), anti-pDE3Aser^{312} (1:250) or an anti β-tubulin antibody (1:1000). Membranes were developed with enhanced chemiluminescence (ECL) solutions.

cAMP measurement

Intracellular cAMP concentrations were quantified using an enzyme immunoassay (EIA) (GE Healthcare). cAMP is measured through the competition between cAMP in a test sample and a fixed quantity of peroxidase-labeled cAMP, for a limited number of binding sites on a cAMP specific antibody. WPs ($2x10^8$/ml) were treated with the indicated agents for selected time intervals and lysed with 10x lysis buffer 1A (2.5% dodecyltrimethylammonium in assay buffer). An aliquot (100µl) of each sample was added to a 96 well plate in triplicate. After a 2 hour incubation at 4°C with gentle shaking, cAMP-peroxidase conjugate (50µl) was then added to each well and incubated for 1 hour at 4°C with gentle shaking. Following incubation, the wells were then washed four times and hydrogen peroxide substrate was added to each well. Absorbance was read at 630nm using a TECAN infinite M200 microplate reader.

Measurement of PDE3A activity

To measure intracellular PDE activity we used a commercially available non-radioactive colorimetric assay. WPs ($5x10^8$/ml) were treated as described, lysed in 2x PDE extraction buffer (150mM NaCl, 50mM HEPES, 20% glycerol (v/v), 10% Igepal (v/v), 1mM, EDTA, 1:200 phosphatase inhibitor cocktail (v/v), protease inhibitor cocktail 1:100 (v/v)) and immediately placed on ice. PDE3A was immunoprecipitated from 500µg of protein lysate using 1µg of anti-PDE3A antibody or matched IgG control. Immunoprecipitates were incubated with 5'-nucleotidase and of cAMP (0.5mM) substrate at 37°C for 1 hour and the production of 5'-AMP measured following the manufacturers instructions. Activity was expressed as fmol AMP/min $1x10^7$ platelets and normalised to control values to account for variations in basal activity between individual platelet donors.

Intravital imaging of in vivo thrombosis

Left carotid artery of anaesthetised mice was exposed and mice injected with Rhodamine G followed by either oxLDL ($2.5mg/kg^{-1}$ body weight) or an equal volume of PBS through the tail vein. [4,5] In some mice, milrinone (10µmol/L) was injected 5 minutes prior to oxLDL injection. 10 minutes after the injection of oxLDL, injury was induced by applying 1x2mm filter paper saturated with anhydrous $FeCl_3$ (10%). Filter paper was placed on the right adventitial surface of the vessel for 1minute then removed. Thrombosis was recorded using high-speed intravital microscopy for up to 40 minutes. The integrated intensity value (Median Fluorescence Intensity) of the thrombus was measured over time and time taken to reach peak was determined. Five individual mice were used for each condition.

Statistics.

Results are expressed as means ± SEM and statistical analyses were undertaken using Prism 6.0 (GraphPad, La Jolla, California). Comparisons between groups were performed by an unpaired, Mann-Whitney U test. P values of less than 0.05 were considered statistically significant.

1. Aburima A, Wraith KS, Raslan Z, et al. cAMP signaling regulates platelet myosin light chain (MLC) phosphorylation and shape change through targeting the RhoA-Rho kinase-MLC phosphatase signaling pathway. *Blood*. 2013;122(20):3533–45.
2. Magwenzi SG, Ajjan RA, Standeven KF, Parapia LA, Naseem KM. Factor XIII supports platelet activation and enhances thrombus formation by matrix proteins under flow conditions. *J. Thromb. Haemost.* 2011;9(4):820–33.
3. Spurgeon BE, Aburima A, Oberprieler NG, Taskén K, Naseem KM. Multiplexed phosphospecific flow cytometry enables large-scale signaling profiling and drug screening in blood platelets. *J. Thromb. Haemost.* 2014;12(10):1733–43.
4. Shen M-YY, Chen F-YY, Hsu J-FF, et al. Plasma L5 levels are elevated in ischemic stroke patients and enhance platelet aggregation. *Blood*. 2016;127(10):1336–45.
5. Badrnya S, Schrottmaier WC, Kral JB, et al. Platelets mediate oxidized low-density lipoprotein-induced monocyte extravasation and foam cell formation. *Arterioscler. Thromb. Vasc. Biol.* 2014;34(3):571–80.

SUPPLEMENTARY FIGURES
Supplementary Material

S1i

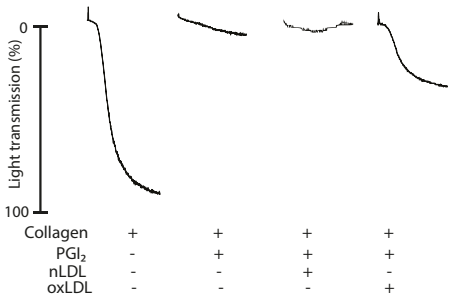

S1ii

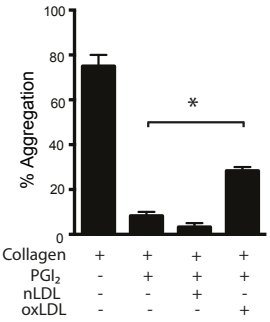

S2

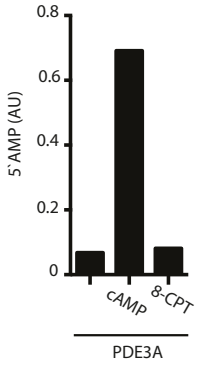

S3

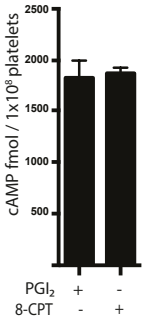

S4

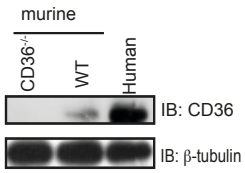

S5

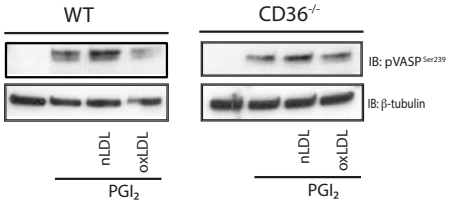

S6

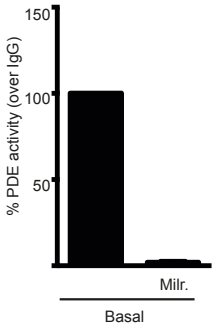

S7

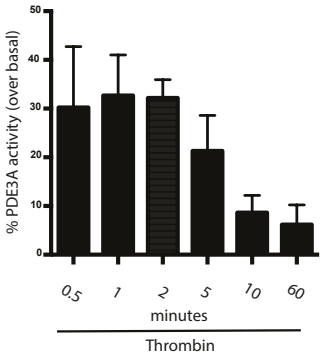

S8

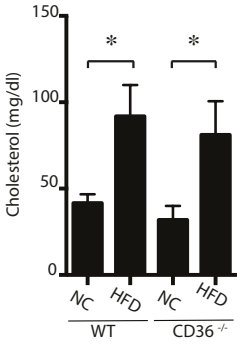

S9i

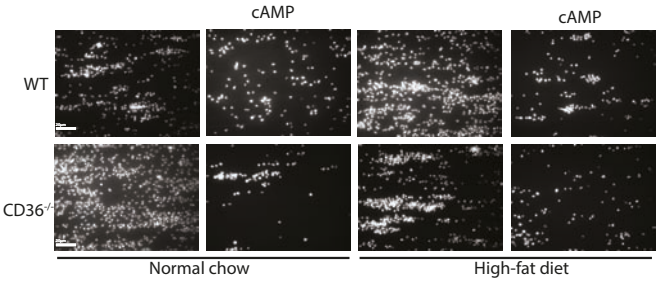

S9ii

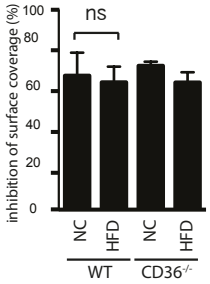

Supplementary Figure 1: OxLDL induces PGI_2 hyposensitivity in platelets.
Washed human platelets (2.5 x 10^8/ml) were incubated with nLDL or oxLDL (50μg/ml) for 2 minutes followed by PGI_2 (20nM) for 1 minute. Collagen-stimulated aggregation was then measured under constant stirring (1000 rpm) at 37°C for 4 minutes. (i) Representative aggregation traces (ii) Data is expressed as percentage aggregation and presented as mean ± SEM (n= 5, * $p < 0.05$ compared to PGI_2 alone).

Supplementary Figure 2: 8-CPT-6-Phe-cAMP is resistant to PDE3a.
PDE3A immunoprecipitates were incubated with cAMP and 8-CPT-6-Phe-cAMP and enzyme activity was measured by production of 5'AMP after 1hour at 37°C. N=2

Supplementary Figure 3: 8-CPT-6-Phe-cAMP increases intracellular cAMP.
Platelets were incubated with PGI_2 (50nM) or 8-CPT-6-Phe-cAMP (50μM) for 5 minutes. Platelets were washed, lysed and intracellular cAMP levels were determined by enzyme immunoassay. Data is presented as mean ± SEM.

Supplementary Figure 4: Immunoblotting of platelet lysates for CD36
Washed human platelets, WT murine platelets and $CD36^{-/-}$ platelets ($5x10^8$/ml) were lysed with Laemmli buffer, separated by SDS-PAGE and immunoblotted with anti-CD36. Representative blot of 3 independent experiments

Supplementary Figure 5: OxLDL modulation of $VASP^{239}$ phosphorylation in murine platelets
Washed murine WT or $CD36^{-/-}$ platelets ($5x10^8$/ml) were treated alone or with nLDL or oxLDL (50μg/ml) for 2 minutes followed by a 1 minute PGI_2 (50nM) incubation. Treated platelets were lysed with Laemmli buffer, separated by SDS-PAGE and immunoblotted with anti-phosphoVASPser^{239} or anti-β tubulin. Representative blot of 3 independent experiments.

Supplementary Figure 6: Immuniprecipitated phosphodiesterase is sensitive to milrinone.
Washed human platelets ($2.5x10^8$/ml) lysed and PDE3A was immunoprecipitated. Enzyme activity measured by cAMP hydrolysis for 1hour at 37°C in the presence and absence of Milrinone (20μM). Data is presented as % activity with basal representing 100% (n=3).

Supplementary Figure 7: Thrombin induced activation of PDE3A as a function of time.
Washed human platelets ($2.5x10^8$/ml) stimulated with thrombin (0.1U/ml) for up to 60 minutes before lysis. PDE3A was immunoprecipitated and enzyme activity measured by cAMP hydrolysis for 1hour at 37°C. Data is presented as % over basal activity (n=3).

Supplementary figure 8: Plasma cholesterol concentrations from WT and $CD36^{-/-}$ mice.
WT and $CD36^{-/-}$ mice were fed either normal chow or High fat diet. Plasma was isolated from whole blood and the concentration of cholesterol measured. Data is expressed as mg/dl cholesterol and presented as mean ± SEM (n=5). * $p<0.05$).

Supplementary figure 9: High-fat diet fed animals show normal platelet sensitivity to PDE-resistant cAMP analogue.
Whole blood of normal chow and high-fat diet fed animals treated with 8-CPT-6-Phe-cAMP (50μM) for 5 minutes was perfused at arterial shear $1000s^{-1}$ for 2 minutes over a collagen (50μg/ml). Images of adherent platelets were taken by fluorescence microscopy. (i) Representative images of arterial flow experiments, (ii) Data expressed as percentage inhibition of surface coverage, mean ± SEM (n=5; ns = not significant).